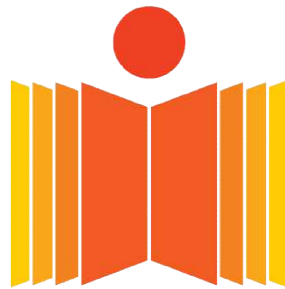# Finite Element Modeling of Weld Deposition Based Additive Manufacturing

Avinash Kumar

A Dissertation Submitted to

Indian Institute of Technology Hyderabad

In Partial Fulfillment of the Requirements for

The Degree of Master of Technology

भारतीय प्रौद्योगिकी संस्थान हैदराबाद

Indian Institute of Technology Hyderabad

Department of Mechanical and Aerospace Engineering

July, 2015

## Declaration

I declare that this written submission represents my ideas in my own words, and where others' ideas or words have been included, I have adequately cited and referenced the original sources. I also declare that I have adhered to all principles of academic honesty and integrity and have not misrepresented or fabricated or falsified any idea/data/fact/source in my submission. I understand that any violation of the above will be a cause for disciplinary action by the Institute and can also evoke penal action from the sources that have thus not been properly cited, or from whom proper permission has not been taken when needed.
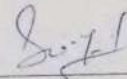
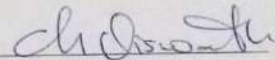Avinash Kumar
14/07/2015

(Signature)


(Avinash Kumar)


(ME13M1020)

# Approval Sheet

This thesis entitled **Finite Element Modeling of Weld Deposition Based Rapid Prototyping**by Avinash kumar is approved for the degree of Master of Technology from IIT Hyderabad.

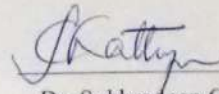Dr. S.Suryakumar
ME, IITH
Supervisor

Dr. Vishwanath Chinthapenta,
ME, IITH
Co-Supervisor

Dr. Chandrika Prakash Vyasarayani
ME, IITH
Examiner

Dr. Subhradeep Chatterjee
MS, IITH,
Chairman

# Acknowledgement

I would like to express my gratitude to Mechanical Engineering department, Indian Institute of Technology Hyderabad which allowed us to take this as a project. Iam highly indebted to our supervisor Dr. S.Suryakumar, whose help, stimulating suggestions and encouragement helped us in all the time of our project and writing this report.

We also wanted to express our gratitude to Dr. Viswanath chinthapenta who has helped me to gain insight.

# Abstract

Additive Manufacturing (AM) is an early design exploration and validation process, in which executable models of a system are created that reflect some subset of properties of interest. It is a process that automatically creates a physical prototype from a three dimensional computer aided design (CAD) model, in a short period of time. It is an indispensable tool for shortening product design and development time cycles. Amongst these, the methods to create metallic prototypes are of special interest to the industrial community and thus research on employing direct metal deposition for the fabrication of fully functional parts and tooling has generated significant interest in recent years. Amongst the deposition based methods using laser, electron beam, arc as the energy source, arc based methods like weld-deposition using Gas Metal Arc Welding (GMAW) are quite suitable for applications requiring high deposition rates.

As the complete part is built by weld-deposition, considerable amount of heat is added to the fabricated object which may result in thermal stresses and distortion. The current work explores the effect of various deposition paths on the residual stresses. It is carried out by Finite Element Modeling of the weld-deposition process. The weld-deposition was modeled as a moving heat source and the deposited metal activated by element birth and death method when the heat source passes over that location. As a complete layer is built by weld-deposition in AM, the work involves multiple pass analysis. In the first part, single wire deposition is presented. This model was later improved for twin-wire welding also in the subsequent chapter. The heat distribution, residual stresses and warping occurring in different patterns is presented.

# Nomenclature

**SLA**        Stereo lithography

**SGC**        Solid Ground Curing

**LOM**        Laminated object manufacturing

**FDM**        Fused deposition modeling

**SLS**        Selective laser sintering

**RP**        Rapid prototyping

**GMAW**        Gas Metal Arc Welding

**CNC**        Computer Numeric Control

# Contents

# Chapter 1

# Introduction

## 1.1 Weld Deposition based Additive Manufacturing

Welding as a deposition process has shown promise for RP metallic parts. Welding is an old and mature technology and is recognized to be used for the development of a cost competitive method for layer-by-layer manufacturing to produce metallic parts and tools. However, welding is a process where high heat input results in large thermal gradient which causes the buildup of residual stresses, distortion and resulting into undesired quality of products. These problems can be reduced to some extent but cannot be eliminated. Post processing can be helpful for producing parts with good accuracy and surface finish. In order to produce accurate parts with less residual stresses, it is recommended to select welding deposition parameters by considering the following criteria necessary of weld based prototyping:

- Depth of Re melt should be shallow (for just reasonable metallurgical bonding).
- Low heat input imparted to the work piece.

## 1.2 Motivation for the Current work

In the depositing process of multi-pass single-layer weld-based rapid prototyping, the rear pass has the stress release effect on the fore passes so non-uniform multi-peak thermal cycle experienced during the depositing is the main cause of the stress release effect. Stress of the last pass plays a significant effect on the residual stress distribution of the whole component. So the residual stress depends on parameters for thermal constraints, deposition parameters and mechanical constraints. So the effect of these parameters needs to be studied to minimize residual stress in part.

Additive manufacturing using single wire 3D welding as a tool has been investigated in the past using FEM and experiments. But little has been done in to explore the twin wire welding as a AM tool. Twin wire welding has slender weld pool the end part of which is ellipsoid, and its HAZ is narrower than that of single wire welding.

## 1.3 Problem Definition

Objective of this study is to investigate the effects of different welding parameters on the deformation produced in the weld-based prototypes. These parameters include mechanical constraints applied; geometry of the heat sink used and interpass cooling time and to find out the optimum parameters under which we get minimum deformation in the substrate plate and hence in our weld-based prototype products.

This dissertation presented an analysis based on a numerical analysis (Finite Element Modeling) for the effects of different deposition and process parameters on welding based rapidprototyping process.

## 1.4 Organization of the report

In Chapter 2 a literate survey on other additive manufacturing process is carried out and advantages of using welding as an AM tool is discussed. Also finite element metrology to simulate welding and mathematical formulation is discussed.

Chapter 3 discusses the single wire modeling and in chapter 4 it is extended to twin wire.

# Chapter 2

# Literature Review

## 2.1  Introduction

Conventional rapid prototyping techniques like SLA,SGC,LOM and FDM have produced a significant impact in design and manufacturing but the application is limited to producing non-metal parts only for visualization and form/fit purpose. SLS produce metal parts but porosity and post processing steps are a major drawback.The post processing methods alters the microstructure, properties and characteristics of the part and also produce significant part shrinkage. Thermal spraying is also an alternative for metal parts and has been used successfully. The application of thermal sprat process to produce parts with high structural integrity and dimensional tolerances is also limited by the presence of porosity. Moreover due to the spray nature of deposition, the inter layer bonding is relatively weak with low inter layer re melting and geometric part with high aspect ratio are also difficult to manufacture.De-lamination due to thermal stresses is also big problem in application of thermal spraying to additive manufacturing.

Welding based deposition has shown promise to produce form/fit/functional parts with high structural integrity and dimensional tolerances. Due to relatively high heat input and large remelting depth the bond layers is very strong. The weld based deposition process can be broadly classified as non transferred mode e.g. Micro casting, or transferred mode e.g. gas metal arc welding.

Welding Based Deposition additive manufacturing technique comprises of all those methods which use welding as a metal deposition process. A welding arc provides the heat to melt the wire, fed by a wire feeding system, while a CNC program developed using the CAD data is used to place welding torch at required position for deposition. This method is also referred to as 3D welding and is still in its experimental phase, as research is in progress to reduce the problem

associated with weld base deposition. This method has the capability of producing form fit and functional parts. A major development is the Hybrid RP system which uses gas metal arc welding and CNC milling. 3D welding and milling is a novel freeform fabrication process and allows the fabrication of metallic prototypes by combined additive and subtractive techniques.

### 2.1.1    Rapid Tooling

Rapid Tooling (RT) is a counterpart of RP to develop molds and tooling for the production of prototype products by using the same processes as those used in rapid prototyping (Gebhardt, 2003). RT can be achieved either through RP model as a pattern to develop a mold or using RP process directly to produce a tool for prototypes. The main distinguishing feature of RT, as compared to traditional tooling, are its much shorter time (one-fifth of conventional tooling), less tooling cost (less than five percent) and wider tolerances as compared to conventional tooling.

### 2.1.2    Rapid Manufacturing

Rapid Manufacturing (RM) or Rapid Production refers to the use of RP technologies to develop end-user products or finished parts. These can be produced directly with rapid prototyping methods or with tools produced by rapid prototyping processes (Gebhardt, 2003).  However there is a degree of uncertainty pertaining to these technologies e.g., built time, part cost and quality of parts developed through RM as compared to those produced from conventional manufacturing technologies. The core advantage of using RM process is its ability to develop customized parts. When the lot size is large the traditional manufacturing technologies are the best option. But when small number of parts has to be produced then traditional technologies never suits for their manufacturing because of high tooling and setup cost.

In this situation RM comes to the surface having ability to produce customized parts in relatively short period of time (Kamrani and Nasr, 2006).

### 2.1.3    Metal Based RP

Rapid prototyping of metallic parts can be carried out through several processes such as droplet based manufacturing, sintering, laser deposition and brazing (soldering). In this context the research work of Ashley (1994) shows that nearly full density prototypes can be achieved

through sintering process. But to attain full density product, post processing is also needed. Although laser deposition method is dimensionally more accurate than sintering, but it causes warpage and some surface finish defects in final product due to the constraining of materials having differing temperature. Soldering and brazing add undesirable bonding materials to the part. Droplet based manufacturing processes are flexible but it also have limits. These can produce full density metallic parts with desired material eliminating cost of post processing. These processes include:

- Welding
- Micro-casting
- Thermal spraying

While Thermal Spraying and Micro-casting have their own advantages, they have many disadvantages and limitations too in terms of lead time and economic aspects. In this study, our focus is only on the Welding process as a mean to produce layer-by-layer additive manufacturing which provide the same properties as our desired final product.

### 2.1.4    Weld Deposition based RP

The commercially available RP machines use the CAD model directly for the development of the product and produce it by layer manufacturing. These Rapid Prototyping (RP) techniques produce models that can mainly be used for visualization of the actual product and cannot be used in place of actual product. The properties of the materials (resins and plastics) that these processes use are far away than the product's actual properties. Presently, the focus of research has been to develop techniques that produce prototypes of the actual product with same shape and material and hence having same properties. Different deposition methods are available for metals but welding has shown potential for additive manufacturing of metallic parts. It has been recognized that welding as a deposition process is more economical and produce full dense metallic parts than other metal based deposition processes.

Now the efforts are being made to develop fully "functionalparts" besides just producing "feel/fit/touch" parts. To establish form-fit and functional testing, the research is being carried out in the field of new and better materials, software development, tolerances and system design

of RP processes. So far many new metal deposition processes have already been developed for the parts with metallic and functional properties due to the need of the market because metallic parts are of specific interest. Welding based AM has good potential in this regard with the best possibility to produce fully functional metallic parts and tools.

### 2.1.5    Welding as a RP Tool

Although welding process is already in use for the fabrication of large components with simple geometry for many years, however such applications of this phenomenon in aerospace industry are quite new.Production of aircraft parts based on titanium and nickel alloys are being manufactured by welding techniques. There is a lot of research available on the optimization of welding parameters for fabrication of simple parts having exceptional weld quality. But this information cannot help out in additive manufacturing by welding. A huge difference exists between the optimized parameters for "welding joints" and as those for "exceptional quality prototype layer". For example the penetration depth, build up height and ratio of both these variables are different for joining by welding and prototyping by welding.

For AM welding process there are some specific requirements to be met. For example low heat input is required for this process in order to retain geometrical features and to avoid high intensity level of residual stresses. Shallow depth of penetration is recommended for better metallurgical bonding between layers.

Different types of welding have been tested for additive manufacturingapplication e.g., Gas Metal Arc Welding (GMAW or MIG welding), Gas Tungsten Arc Welding (GTAW or TIG welding), Electron Beam Welding (EBW), Laser Welding and Variable Polarity Gas Tungsten Arc Welding (VPGTAW).

### 2.1.6    3D Welding

As a production technique, 3-D welding offers significant advantages over conventionalprocessing. These include:

- The potential for robot control of the welding torch allowing large variation in part dimensions and geometry.
- A highly automated system.
- Parts with consistent properties.
- Rapid processing times, hence vastly reduced development times.
- Efficient use of materials.
- Direct production of a metal part- unique amongst current Rapid Prototyping.

## 2.2 Procedure followed for FEM Analysis

The advantage of weak structural to thermal field coupling is employed to break down the complex coupled field thermo-mechanical analysis of welding into two parts. In the first part non-linear transient thermal analysis is performed to predict the temperature history of the domain for complete thermal cycle of single or multi-pass welding.

Quiet elements technique with ambient temperature constraint on the nodes of deactivated elements is employed for modeling of filler material during this work. Nodal constraint is removed at the time of activation of respective element in thermal analysis.

For three dimensional models, time step is constant for each load step during heating andis based on the total heating time and number of elements in axial direction because heat source is supposed to stay on each element at least once.

In the second part, non-linear structural analysis is performed in which temperature history calculated during thermal analysis is applied as body load. Load step time in structural analysis is kept the same as that of the respective thermal load step. In the structural analysis, element of a particular weld bead is activated after four time step.

Figure 1 shows the complete flow chart of this thermal and structural analysis.
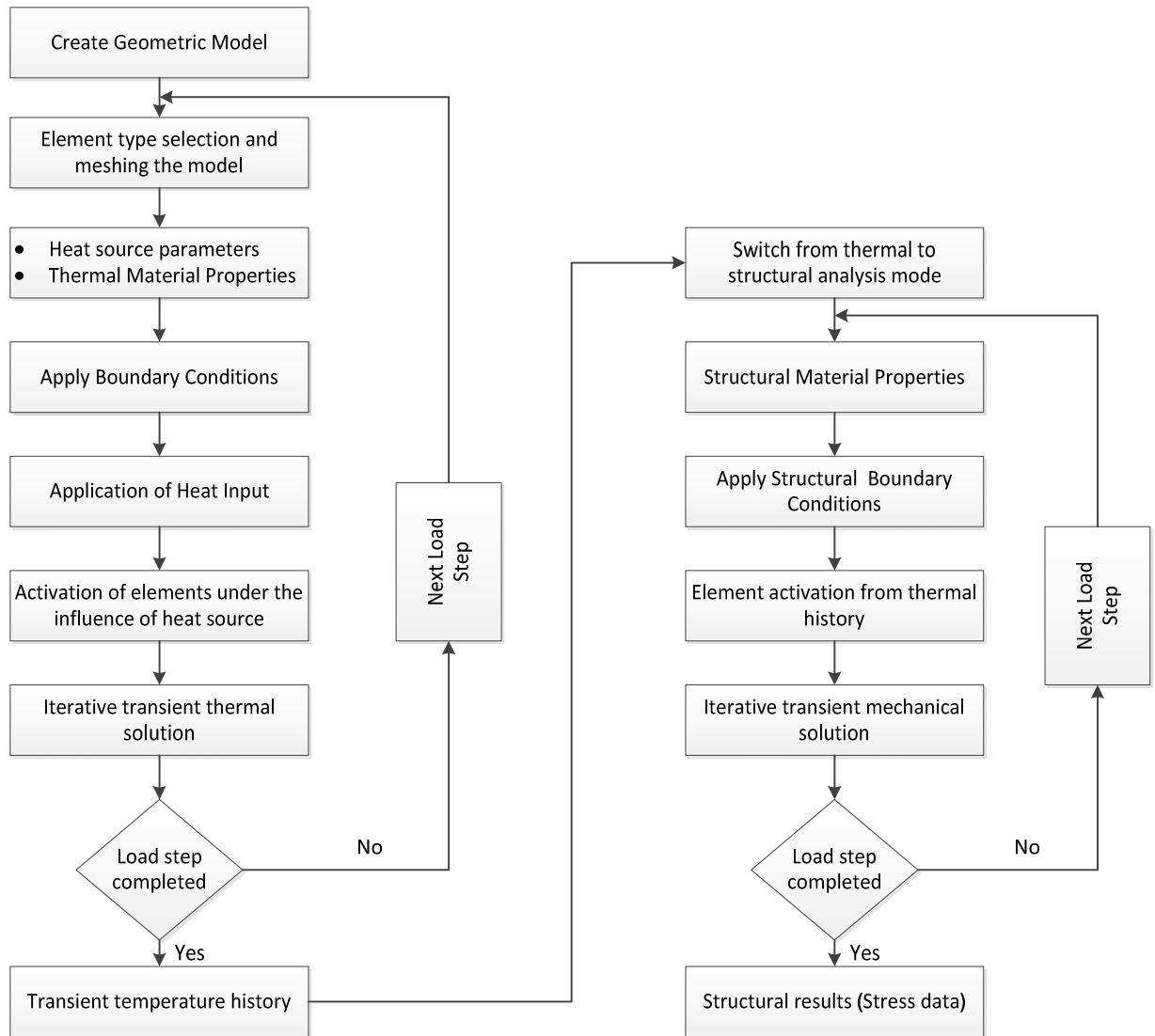
**Figure: 1 Analysis Procedure for Transient Thermal Analysis (Naveen MTech thesis-2014)**

## 2.3  Heat Source Model

A 3D thermal model is developed using a distributed moving heat source, referred as Goldakdouble Ellipsoidal and material addition. The heat distribution within the moving heat source is given by Equation (1), while the applied heat distribution is shown in Figure 3.
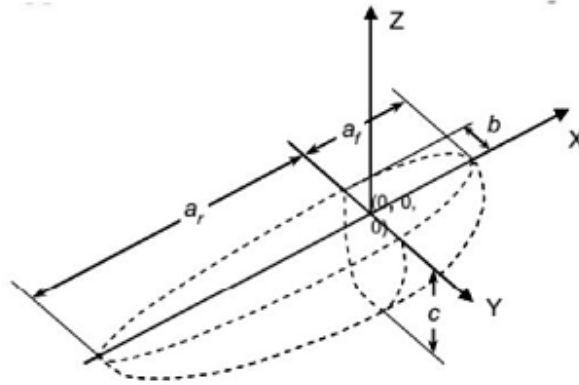
**Figure: 2 Goldak Heat Source Model (Hasan Fawad Junejo-2006)**

$$Q(x, y, z) = \frac{6 * f_i * \sqrt{3} * Q}{\pi\sqrt{\pi}a_i bc} e^{-3(\frac{x^2}{a^2}+\frac{y^2}{b^2}+\frac{z^2}{c^2})} \qquad \text{....(1)}$$

Where,

$$Q = \eta VI$$
$$f_1 + f_2 = 2$$

| S.No. | Parameters | Value |
|-------|-----------|-------|
| 1 | a (mm) | 4 |
| 2 | b (mm) | 6 |
| 3 | $C_1$ (mm) | 3 |
| 4 | $C_2$ (mm) | 7 |
| 5 | $F_f$ | 0.5 |
| 6 | $F_r$ | 1.5 |
| 7 | Voltage (V) | 11.8 |
| 8 | Current (A) | 112 |
| 9 | Welding Speed (mm/sec) | 1.5 |
| 10 | Wire Feed (m/min) | - |

**Table 1: Heat source parameters**

The heat transfer phenomenon is modeled on the following assumptions:

- Heat source overlapping for each pass is 50%
- The Convection present in the molten pool has been modeled by increasing the thermal conductivity to 100 W/m K

9

- The conduction in the base plate is assumed one dimensional

Heat source and deposition parameters are given in Table 1.

The thermal boundary conditions comprise of combined convection and radiation from exposed surface of the substrate and filler material while the diffusion flux is defined at the interface of substrate and the base plate.

The combined heat transfer coefficient for the top exposed surface of the substrate is temperature dependent and is calculated using the following relation

$$h_{eff} = h_{conv} + \varepsilon\sigma(T_s + T_\infty)(T_s^2 + T_\infty^2)$$

The value of $h_{eff}$ changes as the temperature of the surface is changed; the $h_{conv}$ is kept constant at a value of 5.3 W/m$^2$ K, a typical value of free convection from a horizontal plate. The conduction to the base plate is modeled by applying an effective heat transfer coefficient at the base of substrate plate, based on the conductive thermal resistance of the base plate and contact resistance between the base plate and the substrate plate. The thermal resistance based on conduction resistance and contact resistance $\underline{R_c}$, as shown in across the base plate of thickness, $t_b$, is given as

$$R_b = R_c + \frac{t_b}{k}$$

The heat transfer coefficient for base plate conduction is calculated as;
$$h_b = \frac{1}{R_b}$$

## 2.4 Modeling Material addition

Application of FEM to model continuous filler material addition requires special procedures. Two basic approaches are possible, namely, Method of Quiet Element and Inactive Element approach. In the quiet element approach the part of structure which has not been laid as yet is included in the initial computational model but these elements are made passive by assigning them with material properties so that they do not affect the rest of the model. They are given low stiffness i.e. low thermal conductivity, however these cannot be decreased too much since this will result in ill-conditioned matrix. These quiet elements will remain passive until the material

properties are again changed to the actual values and then they become part of the structure and thus simulate time dependent material addition. The second approach i.e. the inactive element method, the model is extended each time the material is added and they are not included as part of initial model. In this paper the quiet elementapproach is used.

## 2.5 Thermo-Mechanical Formulation

For the formulation of thermal model, the basic equation used is the first law ofthermodynamics which states that energy of the system and its surrounding is conserved.

Applying this to a differential control volume V, the heat conduction equation (ignoringthe heat of deformations) is represented as;

$$\rho(T)c(T)\frac{\partial T(x,y,z,\tau)}{\partial \tau} = \nabla q + Q(x,y,z,\tau) \qquad \text{....(2)}$$

Where, Q is the heat generation per unit volume.

The constitutive equation which relates the heat flux and the temperature distribution isthe Fourier law of heat conduction.

$$q = -k(T).A.\nabla T(x,y,z,\tau) \qquad \text{....(3)}$$

Substituting equation (2) in to equation (1) we get,

$$\rho c(T)\frac{\partial T(x,y,z,\tau)}{\partial t} + \nabla k(T).A.\nabla T(x,y,z,\tau) = Q(x,y,z,\tau) \qquad \text{....(4)}$$

Considering a constant thermal conductivity,

$$\rho c(T)\frac{\partial T(x,y,z,\tau)}{\partial t} + k(T).A.\nabla^2 T(x,y,z,\tau) = Q(x,y,z,\tau) \qquad \text{....(5)}$$

The temperature distribution is governed by equation (4).

According to the law of equilibrium, sum of all the forces and moments acting on a body is zero. Mathematically this is written as;

$$\frac{\partial^2 u_i}{\partial t^2} = \frac{1}{\rho}\frac{\partial \sigma_{ij}}{\partial x_j} + F_i \qquad \text{....(6)}$$

Where, i =1, 2, 3

11

For linear thermo-elastic problems, the stress-strain relationship in terms of Lame's constant is given as,

$$\sigma_{ij} = \delta_{ij}\lambda\varepsilon_{kk} + 2\mu\varepsilon_{ij} - \delta_{ij}(3\lambda + 2\mu)\alpha T \quad\quad ....(7)$$

The strain-displacement relationship is,

$$\varepsilon_{ij} = \frac{1}{2}(\frac{\partial u_i}{\partial x_j} + \frac{\partial u_j}{\partial x_i}) \quad\quad ....(8)$$

Substituting equation (7) and (8) in equation (6) and after simplifying, we get

$$\frac{\partial^2 u_i}{\partial t^2} = (\lambda + \mu)\frac{\partial \varepsilon_{kk}}{\partial x_i} + \mu\nabla^2 u_i - (3\lambda + 2\mu)\alpha\frac{\partial T}{\partial x_i} + F_i \quad\quad ....(9)$$

The term $(3\lambda + 2\mu)\alpha\dfrac{\partial T}{\partial x_i}$ provides coupling between equations (9) and (5). The temperatures are calculated from equation (5) and are applied as body loads through $(3\lambda + 2\mu)\alpha\dfrac{\partial T}{\partial x_i}$ .in Equation (9). The calculated displacements are used to get stress and strain using equation (7) and (8) respectively.

## 2.6 Finite Element Formulation

For isotropic material, temperature distribution given in equation (5) can be rewritten in expanded form as;

$$\rho C\frac{\partial T}{\partial t} = \frac{\partial(K\frac{\partial T}{\partial x})}{\partial x} + \frac{\partial(K\frac{\partial T}{\partial y})}{\partial y} + \frac{\partial(K\frac{\partial T}{\partial z})}{\partial z} \quad\quad ....(10)$$

Matrix form of equation (5) is;

$$\rho C\frac{\partial T}{\partial t} = \{L\}^T ([D]\{L\}T) + Q \quad\quad ....(11)$$

Where, $L = \begin{bmatrix} \dfrac{\partial}{\partial x} \\ \dfrac{\partial}{\partial y} \\ \dfrac{\partial}{\partial z} \end{bmatrix}$

$$D = \begin{bmatrix} K & 0 & 0 \\ 0 & K & 0 \\ 0 & 0 & K \end{bmatrix}$$

Where, L is the gradient vector while D is the material stiffness matrix.

Employingconvective boundary conditions at the surface enclosing the volume "V", it gives;

$$[q]^T \, \eta = h_f (T_B - T) \qquad \text{....(12)}$$

Where, $\eta$ is a unit vector perpendicular to the surface.

Taking the boundary effects into account, the Equation (11) becomes;

$$\rho C \frac{\partial T}{\partial t} = \{L\}^T \{[D]\{L\}T\} + Q + h_f (T_B - T) \qquad \text{....(13)}$$

The differential Equation (11) when multiplied by T and integrated over the control volume using the boundary conditions yields

$$\int_V (\delta T \rho C \frac{\partial T}{\partial t}) dv + \int_V \delta T \{L\}^T [D]\{L\} T dv = \int_v \delta T Q dv + \int (\delta T h_f (T_B - T)) dA \qquad \text{....(14)}$$

Let for any element E, the temperature is represented as

$$T = [N] \delta T_E \qquad \text{....(15)}$$

Were $T_E$ is the nodal temperature and [N] is the matrix of element shape functions. The equation is valid for all permissible $\delta T_E$ .If

$$B = [L][N] \qquad \text{....(16)}$$

Where B is the derivative of shape functions Substituting Equations (14), (15) and (16) in Equation (13), yields

$$\rho \int_V (C[N][N]^T \{T\}) dv + \int_V ([B]^T [D][B]\{T_E\}) dv = \int_V ([N]Q) dv + \int_A [N] h_f (T_B - [N]^T \{T_E\})\alpha \quad \text{....(17)}$$

 Equation (17) containing nodal temperatures can be written in a condensed form as,

$$[C]\{T_E\}+[K]\{T_E\}=\{F_E\} \qquad \qquad \ldots.(18)$$

Where,

$[C] = \rho \int_V (C[N][N]^T)dv$ Specific heat matrix

$[K] = \int_V ([B]^T[D][B])dv + \int_A h_f[N][N]^T dA$ Thermal Conductivity matrix

$\{F_E\} = \int_V Q[N]dv + \int_A h_f T_B[N]dA$ Heat generation and convection matrix

Equation (18) is an elemental equation with vector $\{T_E\}$ containing unknown nodal temperatures. A system of equations is obtained by assembling the individual elemental equations. The system of equation is then solved using appropriate solution technique e.g. Newton-Raphson for the unknown nodal temperature. The finite element form of equation (4) can be derived using the principle of virtual work. The principle of virtual work states that a virtual (very small) change of the internal strain energy must be offset by an identical change in external work due to applied load, mathematically this is written as;

$$\delta U = \delta P \qquad \qquad \ldots.(19)$$

Where

U=Internal strain energy or internal work

P = external work, like due to inertia effect

δ = virtual operator

The virtual strain energy is given as,

$$\delta U = \int_V \{\delta\varepsilon\}^T \{\sigma\}d\{V\}dv \qquad \qquad \ldots.(20)$$

$\varepsilon$ = Strain vector

$\sigma$ = Stress Vector

V = Volume of element

From the theory of basic solid mechanics,

$$\sigma = D\varepsilon^{el} \qquad \qquad \text{....(21)}$$

And

$$\varepsilon = \varepsilon^{el} + \varepsilon^{th} \qquad \qquad \text{....(22)}$$

Where,

$\varepsilon$ = Total strain

$\varepsilon^{el}$ = Elastic strain

$\varepsilon^{th}$ = Thermal strain

D=Material stiffness matrix

The thermal strain vector for an isotropic medium with temperature dependent coefficient of thermal expansion is given as

$$\varepsilon^{th} = \nabla\alpha(T) \qquad \qquad \text{....(23)}$$

$\nabla\alpha(T)$, is the difference between the reference temperature and actual temperature. Substituting equations (20) and (21) in equation (19) yields

$$\delta U = \int_{V} (\{\delta\varepsilon\}^{T}[D]\{\varepsilon\} - \{\delta\varepsilon\}[D]\{\varepsilon\}^{th})dV \qquad \qquad \text{....(24)}$$

The strain is related to nodal displacement by the following relations

$$\{\varepsilon\} = [B]\{u\} \qquad \qquad \text{....(25)}$$

For a constant displacement, virtual straining energy is given as;

$$\delta U = \{\delta u\}^{T} \int_{V}[B]^{T}[D][B]dV\{u\}dV - \{\delta u\}^{T}\int_{V}[B]^{T}[D][\varepsilon^{th}]dV \qquad \qquad \text{....(26)}$$

The external virtual work due to inertia forces is formulated as;

$$\delta P = -\int_{V}\{\delta w\}^{T}\frac{\{F^{a}\}}{v}dV \qquad \qquad \text{....(27)}$$

Where,

w=displacement vector of a general point

According to Newton second law of motion

$$\frac{\{F^a\}}{v} = \rho\frac{\partial^2\{w\}}{\partial\tau^2}$$

<div align="right">....(28)</div>

If the displacement within the element is related to nodal displacement by

$$\{w\}=[N]\{u\}$$

<div align="right">....(29)</div>

Then equation (27) can be re-written as

$$\delta P = \{\delta u\}\rho\int [N]^T[N]\frac{\partial^2 u}{\partial\tau^2}dV$$

<div align="right">....(30)</div>

Substituting equations (27) and (30) in equation (17), yields,

$$\{\delta u\}^T = \int_V [B]^T[D][B]\{u\}dV - \{\delta u\}^T\int_V [B]^T[D][\varepsilon^{th}]dV = -\{\delta u\}\rho\int_V [N]^T[N]\frac{\partial^2 u}{\partial\tau^2}dV$$

<div align="right">....(31)</div>

$\{\delta u\}^T$, vector is a set of arbitrary virtual displacement common in all terms, the condition required to satisfy equation (31) reduces to

$$[K_e]-[F_e^{th}]=[M_e]\ddot{u}$$

<div align="right">....(32)</div>

Where,

$[K_e] = \int_V [B]^T[D][B]dV$ Element Stiffness Matrix

$[F_e^{th}] = \int_V [B]^T[D][\varepsilon^{th}]dV$ Element Thermal Load Vector

$[M_e] = \rho\int_V [N]^T[N]dV$ Element Mass Matrix

# Chapter 3

# Finite Element Modeling of Single Wire Weld Deposition

## 3.1 Finite Element Model

The commercial FE software ANSYS is used to develop the model which, in thisstudy, is used to investigate the effects of different process parameters on deformation and residual stresses of the substrate plate. A sequentially coupled, thermo-mechanical FE model is being developed, in which the transient temperature distribution from thermalanalysis was applied as body load to the structural model.

The basic geometry of the model comprises of a rectangular substrate plate of dimensions LxWxTS mm as shown in Figure 3, bolted at the four corners to a support plate of same dimensions. The deposition in the original model consists of five successively deposited rows, with the length of each row equal to LD mm, and in between rows the model was allowed to cool down for 4 seconds (i.e. the interpass cooling time).

The FE model consists of 10700, 3D Solid-70 element with mid side nodes.SOLID70 has a three-dimensional thermal conduction capability. The element has eight nodes with a single degree of freedom, temperature, at each node. The element is applicable to a three-dimensional, steady-state or transient thermal analysis. In structural analysis element type is changed to an equivalent structural element SOLID45.SOLID45 is used for the three-dimensional modeling of solid structures. The element is defined by eight nodes having three degrees of freedom at each node: translations in the nodal x, y, and z directions. The element has plasticity, creep, swelling, stress stiffening, large deflection, and large strain capabilities.

Mesh size is biased toward the deposition area. As the heat flow is dominantly in direction transverse to welding, therefore the mesh size is 1mm across the welding direction and 1 mm along the welding direction. The time step size is determined by dividing the length of heat source by welding speed.

The basic geometry of the model comprises of a rectangular substrate plate on which weld metal has been deposited to form a slab as shown in Figure 3. Initially a single layer has been modeled but the subroutine can be used to deposit multiple layers. The finite element model uses an 8 noded solid element with ability to model material addition feature during the analysis. A small element size is used in areas across the welding directions but a relatively large element size is used along the welding directions. A fine mesh is used in areas near the heat affected zone but the mesh becomes coarser in regions away from the welding zone.

The base plate is assumed to be very thick so it acts like a rigid support to substrate plate, not allowing any point on substrate base to move in to the base plate or 'Y' direction but will not oppose any motion in 'Y+' direction, when the substrate plate is unbolted. The base plate is not modeled as separate geometry rather its effect is modeled by 2 noded contact element Contac12.This element represents two surfaces which may maintain or break physical contact and may slide relative to each other. The element is capable of supporting only compression in the direction normal to the surfaces and shear in tangential direction. A normal stiffness is defined for the element based on the stiffness of the surface in contact.

The base plate is modeled by generating additional set of nodes, coincident with the nodes at the bottom of substrate. These additional set of nodes represents the top of base plate and are completely constraint during the entire solution to simulate a rigid base.Contac12 elements are generated between these coincident set of nodes with one node attached to rigid base while the other node attached to moveable substrate. Since these node sets are coincident therefore they represents an initial perfect structural close gap condition or an initial perfect structural contact

between the substrate and base plate. As the gap is initially close therefore the nodes corresponding to bottom of the substrate cannot move down.

During simulation all DOF's of all the nodes at the base of the substrate are completely constrained to avoid any warping. As the deposition ends and the plate cools down to room temperature the plate is unbolted by removing the constrains only from the nodes representing the base of substrate plate while the nodes representing the base plates were kept completely constraint. The unbolted deflection was obtained by solving an additional load step.
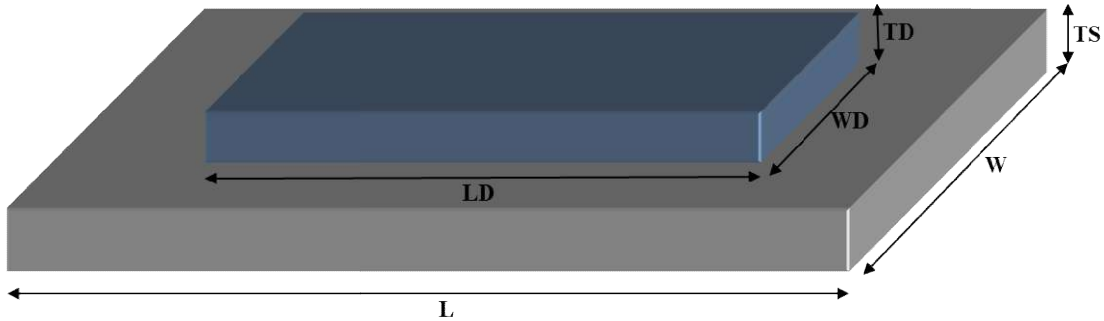


**Figure 3: Model Geometry**

| S. No. | Parameters | Value |
|--------|------------|-------|
| 1 | L (mm) | 70 |
| 2 | W (mm) | 60 |
| 3 | TS (mm) | 7 |
| 4 | LD (mm) | 50 |
| 5 | WD(mm) | 42 |
| 6 | TD(mm) | 3 |

**Table 2: Geometry parameters**

Three deposition sequences are to be evaluated as shown in Figure 4.

1. Long Parallel Raster

2. Zigzag

3. Spiral

19
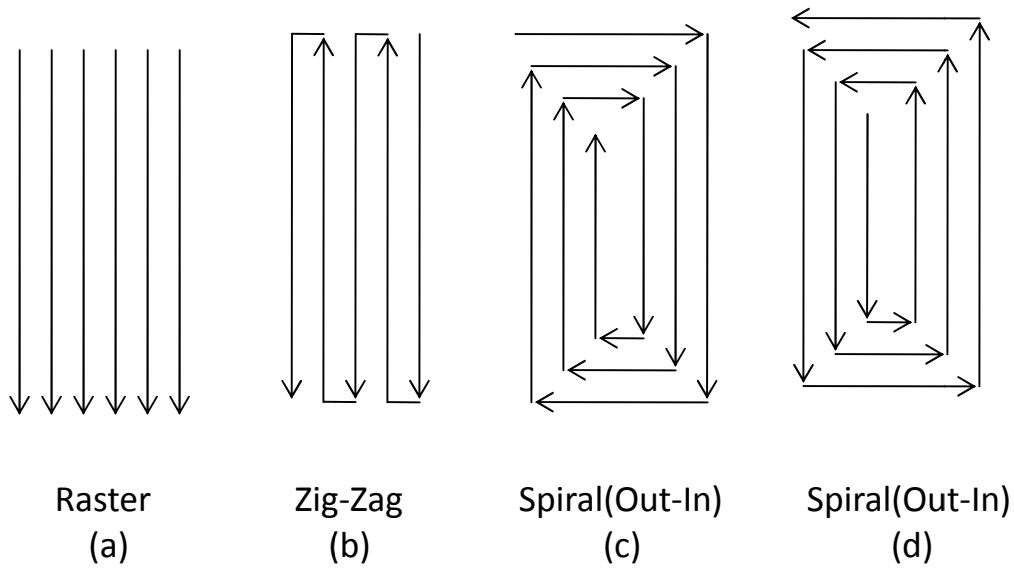
Figure 4: Deposition Patterns

## 3.2 Single Wire Zigzag Simulation

### 3.2.1 Thermal Simulation and Result

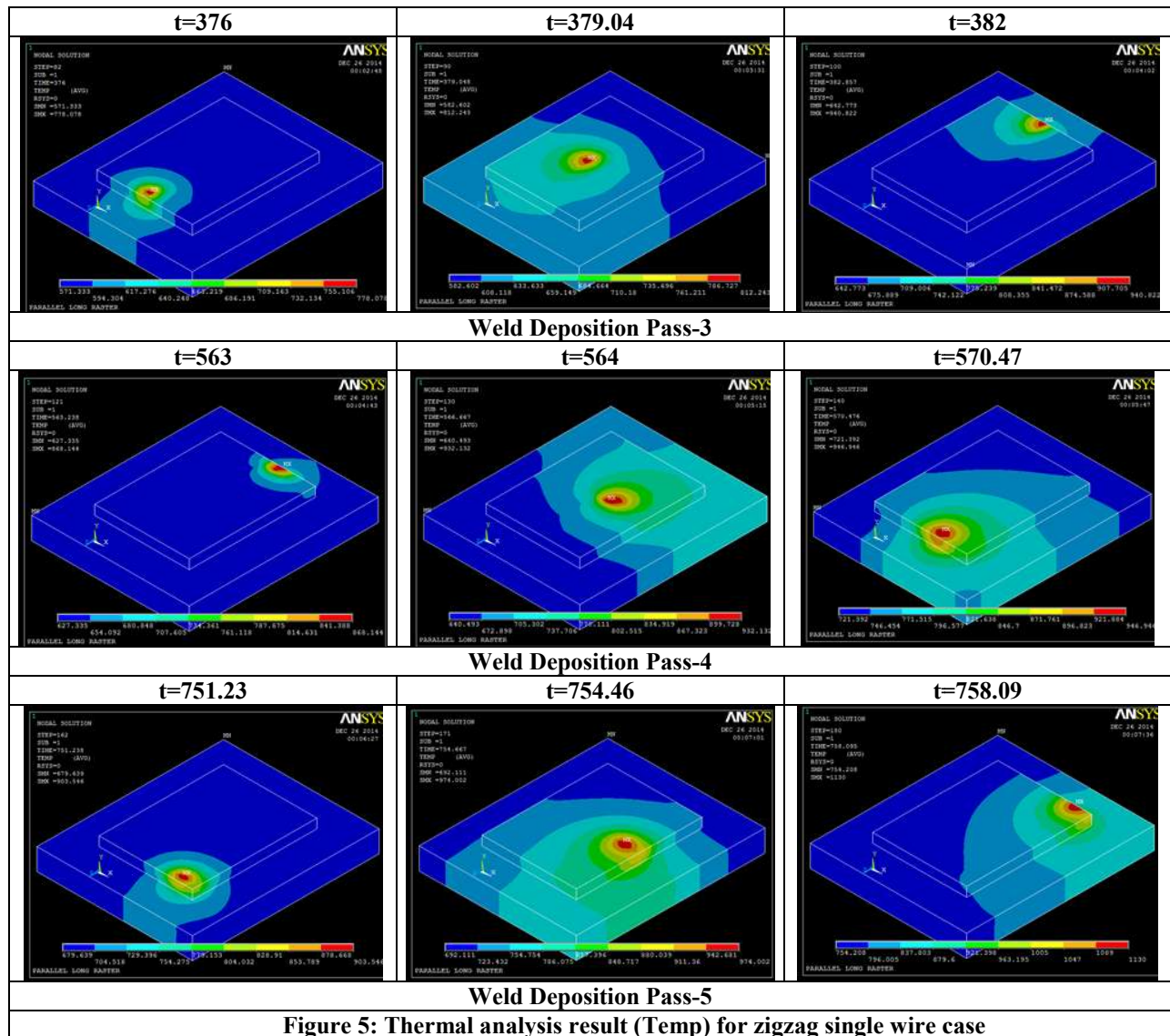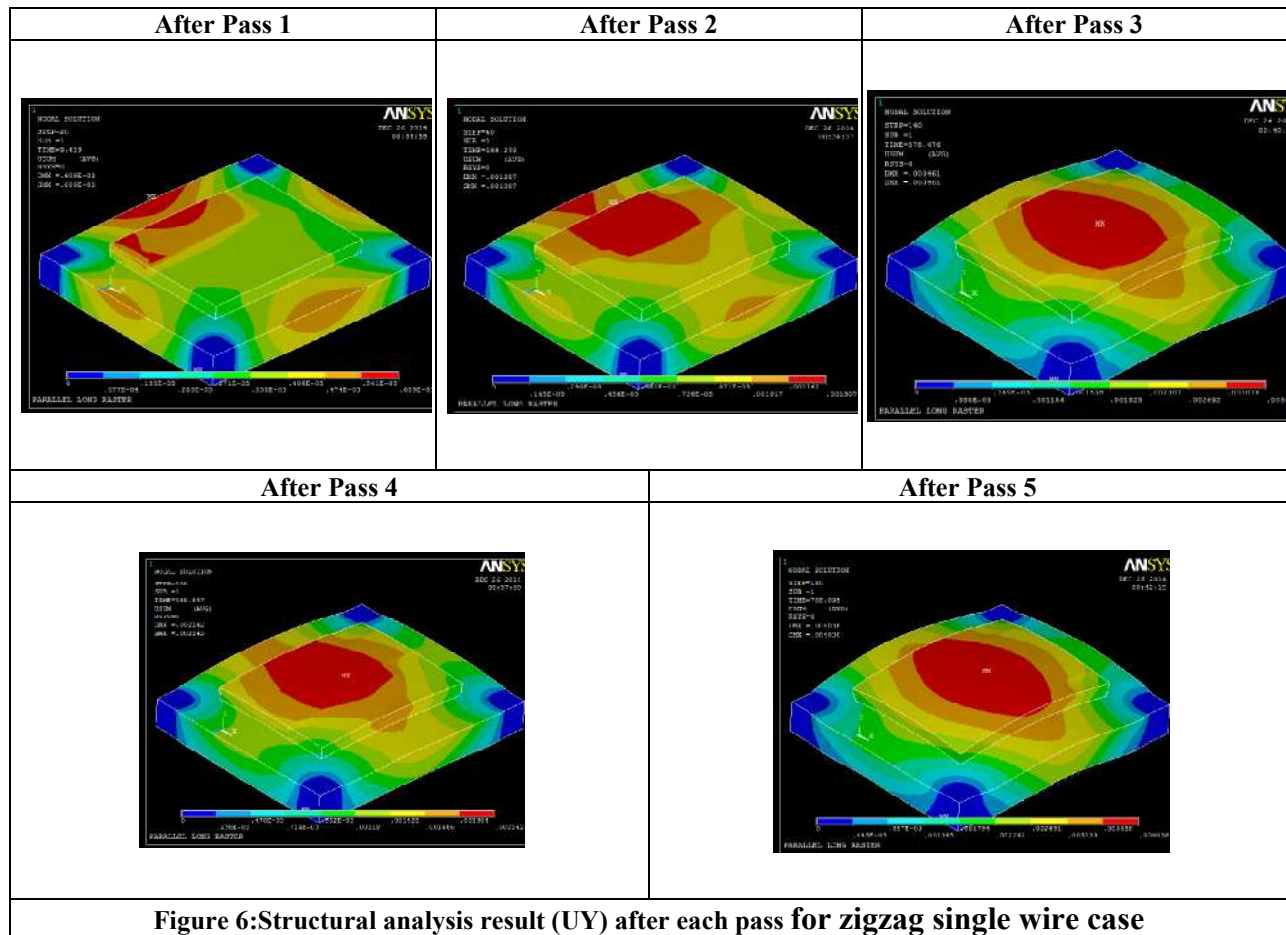Temperature distribution at various time steps (seconds) is shown in Figure 5.
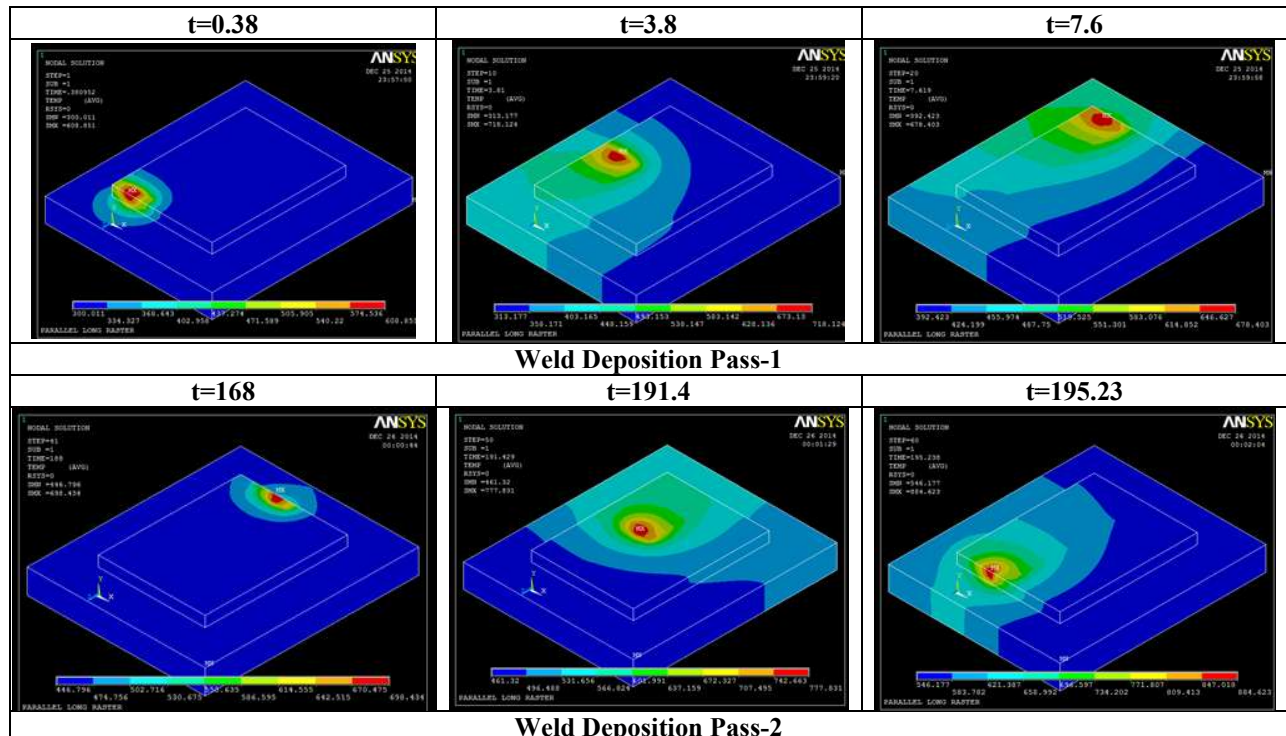
| t=376 | t=379.04 | t=382 |
|---|---|---|
|  |  |  |
| **Weld Deposition Pass-3** | | |
| t=563 | t=564 | t=570.47 |
|  |  |  |
| **Weld Deposition Pass-4** | | |
| t=751.23 | t=754.46 | t=758.09 |
|  |  |  |
| **Weld Deposition Pass-5** | | |
| **Figure 5: Thermal analysis result (Temp) for zigzag single wire case** | | |

### 3.2.2 Structural Simulation and Result

Similarly, deflection obtained from structural analysis at the end of every weld deposition pass is shown in Figure 6.

| After Pass 1 | After Pass 2 | After Pass 3 |
|---|---|---|
|  |  |  |

| After Pass 4 | After Pass 5 |
|---|---|
|  |  |

**Figure 6:Structural analysis result (UY) after each pass for zigzag single wire case**

From these preliminary simulations some trends can be identified as mentioned below.

The Peak temperature for each point is same but the time at which this peak occurs is dissimilar.

- When the heat source is close to any of point under consideration, the temperature of that point is relatively higher.

- The magnitude of thermal cycling is not symmetric but depends upon the relative position of the heat source.

- During deposition the thermal cycling results in compressive reaction forces at the plate edges.

- The reaction causes the substrate plate to deflect upward. This upward deflection has a maximum at the mid-length of the plate and decreases on both sides.

## 3.3 Summary

In this model only elastic material parameters were used so the stresses and deflection results observed were too high which were not realistic. Also the base material properties and substrate properties were taken same. So it was not possible to model different welding wire material parameter effect. A model is developed in next chapter where we change the material property of weld at every step as the deposition is done. All the material parameters of base plate and weld are same except their yield strengths. Among various plasticity model BISO (Bilinear Isotropic Hardening) is found to be most suitable for our present case.

# Chapter 4

# Twin Wire Finite Element Modeling

## 4.1 Introduction

The main aim of the work in this chapter is to simulate the metal deposition using finite element method with specific application to additive manufacturing using twin wire arc welding. The validity of the model depends on accurate prediction of temperature and fusion zone. The temperature histories up to 5 passes are shown in Figure 8, Figure 10 and Figure 12.

It is also observed that at the start of each pass, due to inter pass cooling, the temperature of all the nodes under consideration are almost same. Interpass cooling thus plays a major role in controlling the operational substrate temperature which in turn will control the surface quality of the product.

## 4.2 Modeling Twin Wire

Based on single wire double ellipsoid heat source model is modified, and a heat source model which can apply to calculate the twin wire welding temperature field is put forward.Twin Wire heat source is modeled by adding the heat equation for two single wires as shown in figure below. The distance between the heat sources is taken as 6 mm. Heat source equation (1) is calculated twice in every time step. By the geometry of model y and z in equation is same for both heat sources. So now Q is calculated as,

$$Q(x,y,z) = \frac{6*f_i*\sqrt{3}*Q}{\pi\sqrt{\pi}a_ibc}\left(e^{-3\left(\frac{x1^2}{a^2}+\frac{y^2}{b^2}+\frac{z^2}{c^2}\right)}+e^{-3\left(\frac{(x1-Gap)^2}{a^2}+\frac{y^2}{b^2}+\frac{z^2}{c^2}\right)}\right)$$

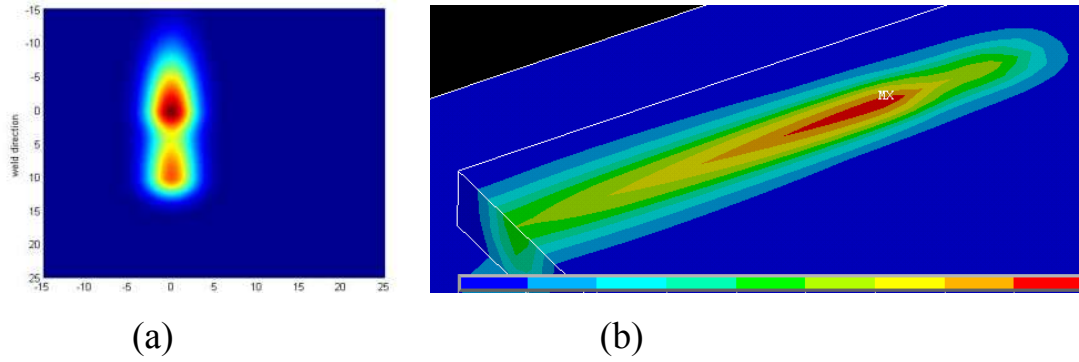A mat-lab implementation and FEM implementation is shown in Figure 7,

Figure 7:Twin wire heat source (a) Mat Lab (b) Finite Element Modeling

Effect of arc deflection is not modeled. Though it can be modeled using the equation given below as suggested by Q.G.Meng et.al 2005,

$$Q = \frac{6\sqrt{3}\eta Q f_f cos^2\beta}{\pi\sqrt{\pi}a_f bc} e^{-3\left\{\left(\frac{x^2}{\left(\frac{a_f}{cos\beta}\right)^2}\right)+\left(\frac{y^2}{b^2}\right)+\left(\frac{z^2}{\left(\frac{c}{cos\beta}\right)^2}\right)\right\}}$$

Where $\beta$ is the deflecting angle

The temperature-dependent material properties of the substrate are used for depositing metal. The filler metal was mild steel with AWS designation as ER70S-6 wire while the base plate is mild steel. Complete ranges of material properties for different temperatures are given in table 3.

| Temperature | °C | 0 | 300 | 600 | 900 | 1200 | 1500 | 1800 | 2100 | 2400 | 2700 |
|---|---|---|---|---|---|---|---|---|---|---|---|
| Thermal Conductivity | W/m °C | 50 | 47 | 40 | 27 | 30 | 35 | 37 | 40 | 42 | 42 |
| Specific Heat Capacity | J/(Kg°C) | 400 | 450 | 500 | 550 | 600 | 650 | 700 | 750 | 800 | 850 |
| Poisson's ratio | | 0.26 | 0.27 | 0.28 | 0.30 | 0.33 | 0.35 | 0.38 | 0.40 | 0.42 | 0.42 |
| Thermal Expansion Coeff. | $10^{-6}$/°C | 12 | 12 | 12 | 12 | 12 | 12 | 12 | 12 | 12 | 12 |
| Modulus of Elasticity | GPa | 250 | 250 | 200 | 180 | 150 | 65 | 55 | 45 | 35 | 25 |

**Table 3: Material Properties**

## 4.3 Pattern Analysis

Three patterns are analyzed while the geometry and other parameters are same.These parameters are given in table 4.

| Case No. | Path | Geometry Parameters | Heat Source Parameters | Mechanical Constraints | Deposition parameters |
|---|---|---|---|---|---|
| 1 | Raster | Table 2 | Table 1 | Bolted on Corners 9X9 mm | Bead Width:10 mm Inter pass :NO |
| 2 | Zigzag | Table 2 | Table 1 | Bolted on Corners 9X9 mm | Bead Width:10 mm Inter pass :NO |
| 3 | Spiral | Table 2 | Table 1 | Bolted on Corners 9X9 mm | Bead Width:10 mm Inter pass :NO |

**Table 4: Case Study Parameters**

### 4.3.1    Raster Pattern

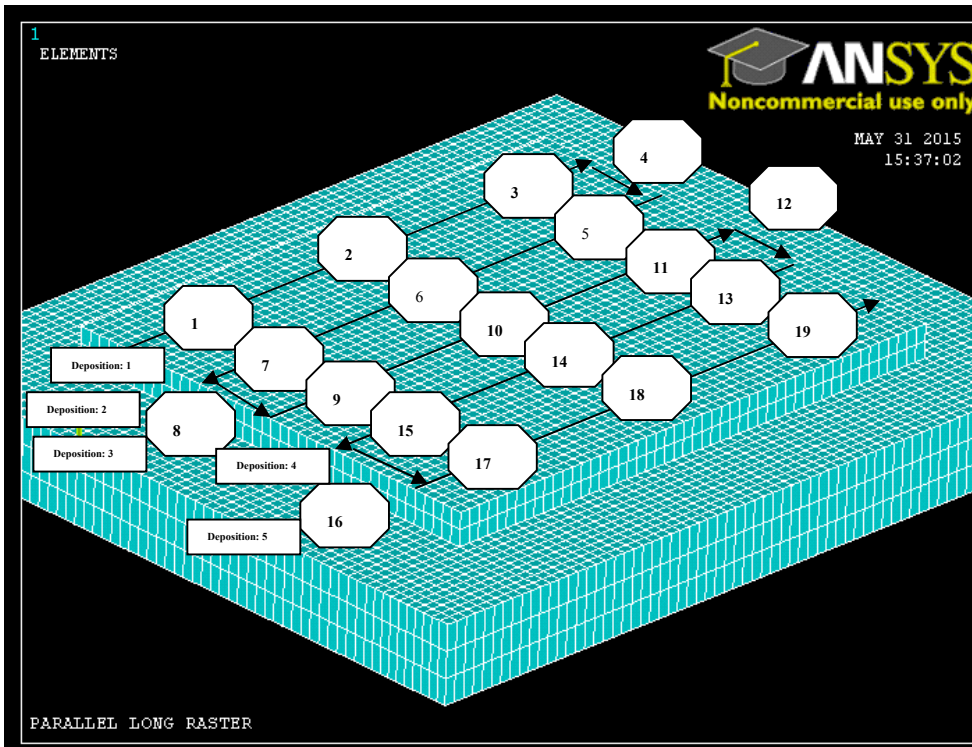Thermal and Structural results for instance marked Figure 8 for each pass/deposition are shown subsequently.
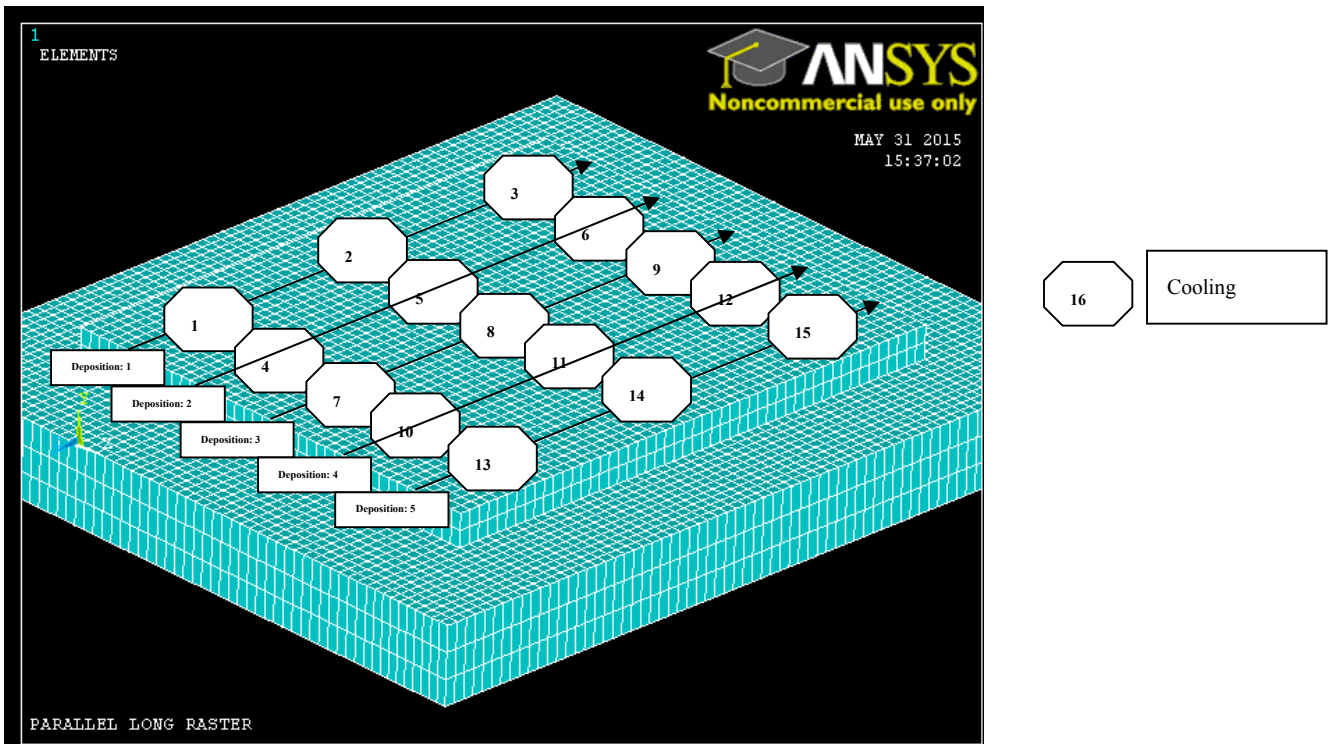


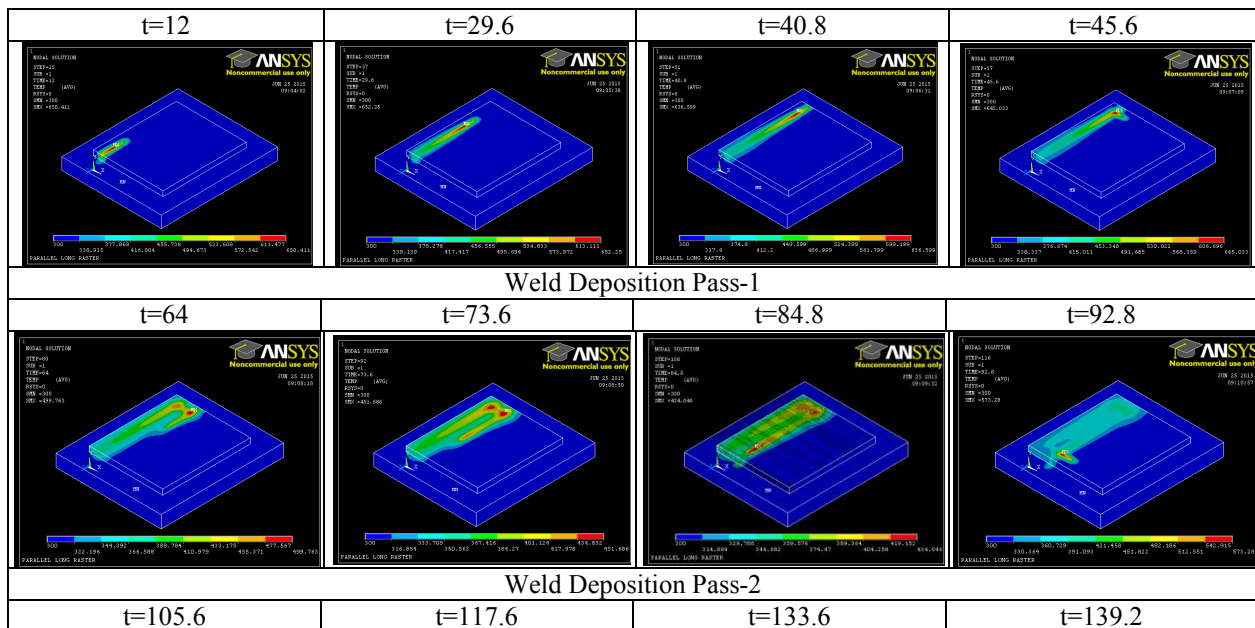**Figure 8:Finite element mesh and raster pattern**

| t=11.33 | t=24 | t=33.33 |
|---|---|---|
|  |  |  |
| Weld Deposition Pass-1t= | | |
| t=48.66 | t=61.33 | t=70.66 |
|  |  |  |
| Weld Deposition Pass-2 | | |
| t=89.33 | t=96 | t=113.33 |
|  |  |  |
| Weld Deposition Pass-3 | | |
| t=126.66 | t=136.66 | t=148.33 |
|  |  |  |
| Weld Deposition Pass-4 | | |
| t=163.33 | t=174.66 | t=182.66 |

| t=11.33 | t=24 | t=33.33 |
|---------|------|---------|
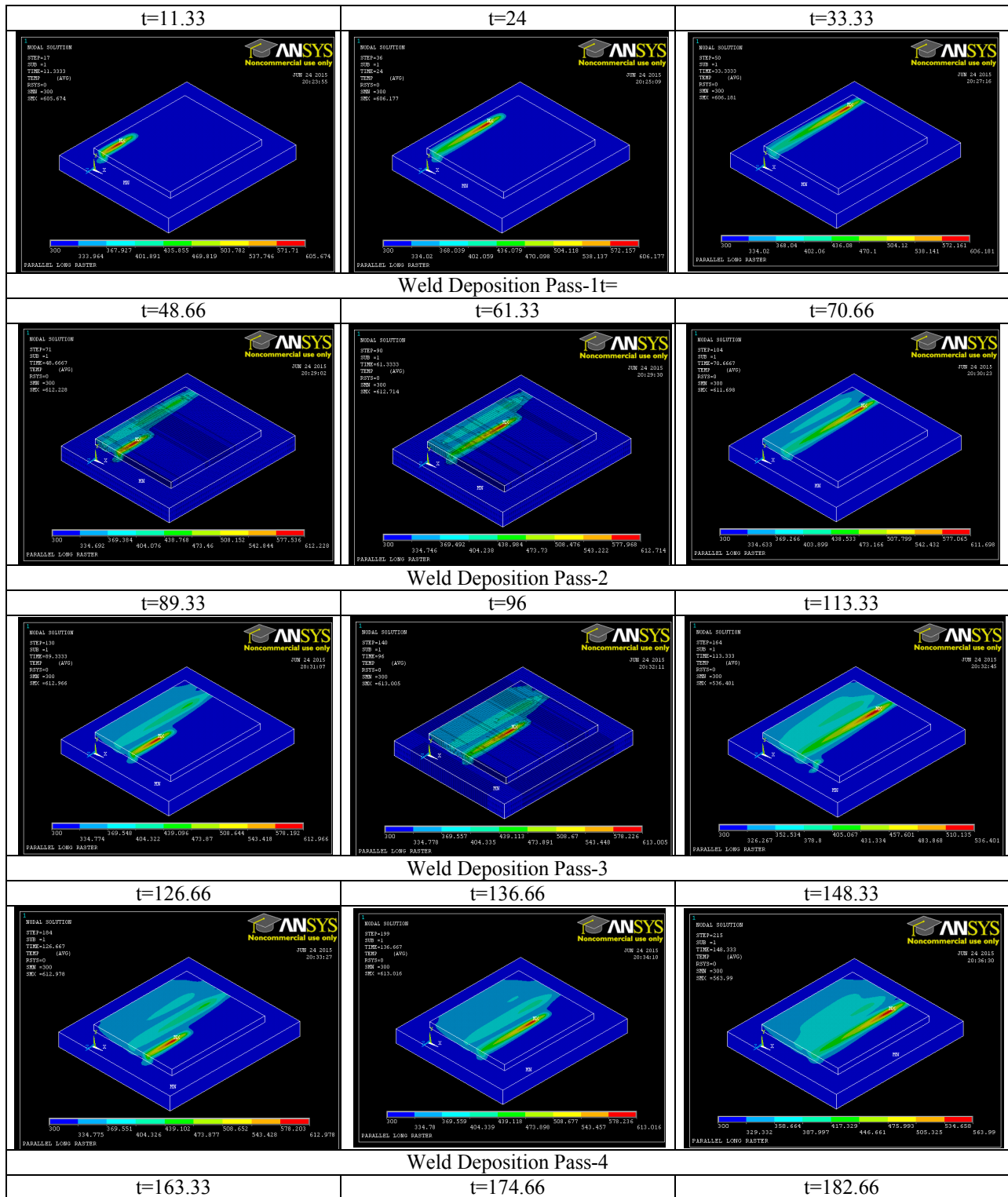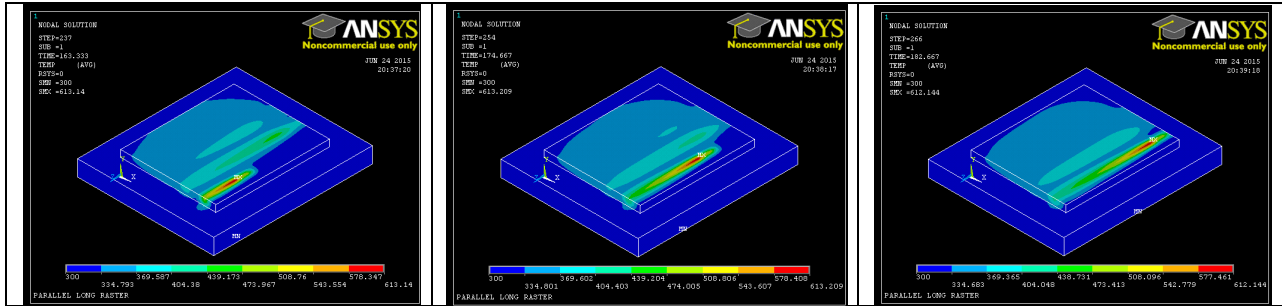


Weld Deposition Pass-5

**Figure: 9 Thermal analysis result (Temp) for Raster Twin wire case**

| t=11.33 | t=24 | t=33.33 |
|---------|------|---------|



Weld Deposition Pass-1
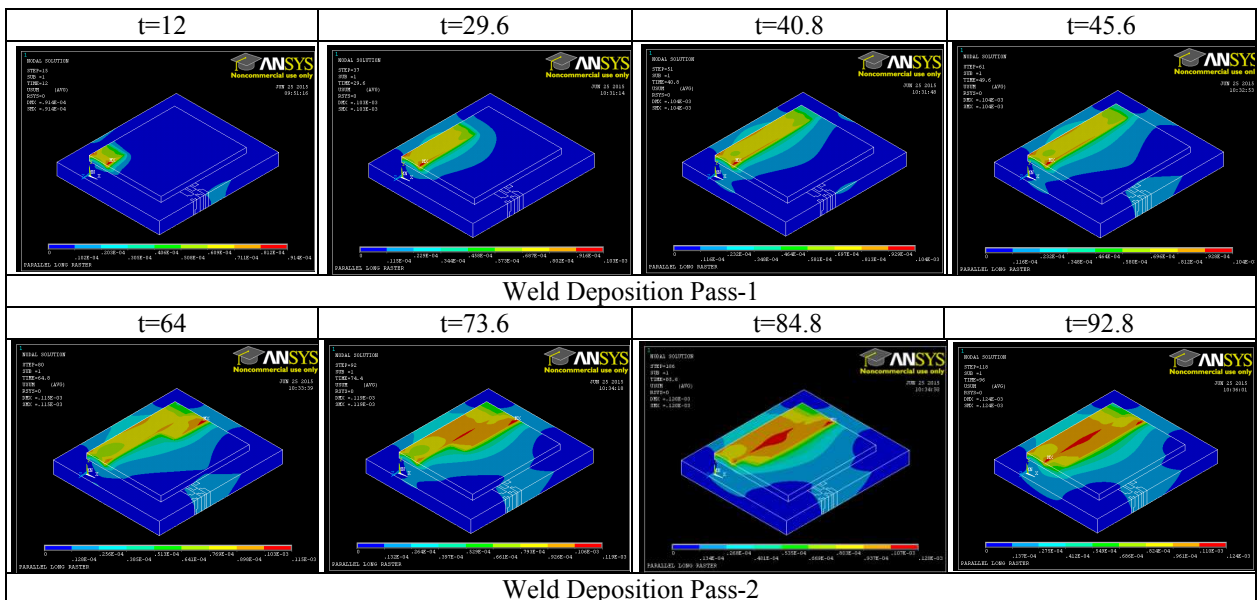
| t=48.66 | t=61.33 | t=70.66 |
|---------|---------|---------|



Weld Deposition Pass-2

| t=89.33 | t=96 | t=113.33 |
|---------|------|----------|



Weld Deposition Pass-3

| t=126.66 | t=136.66 | t=148.33 |
|----------|----------|----------|

28
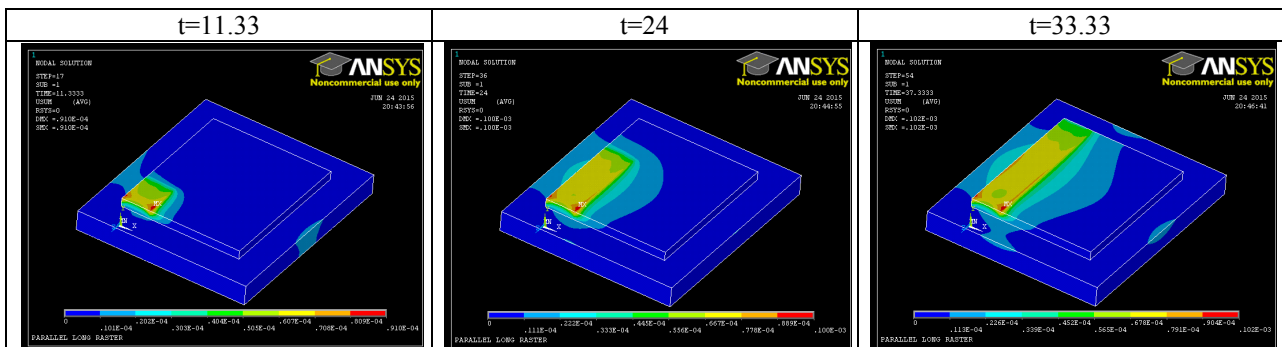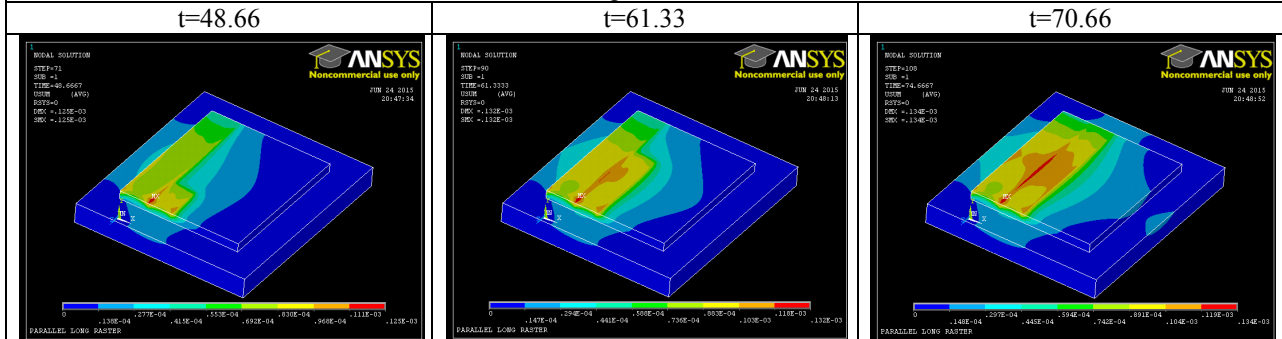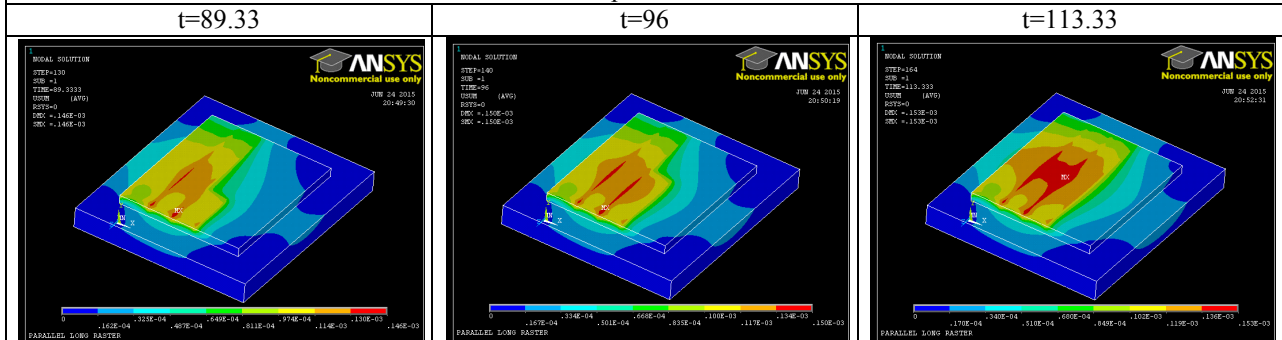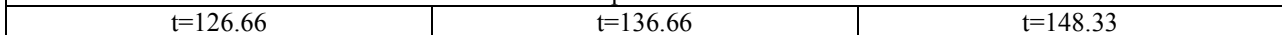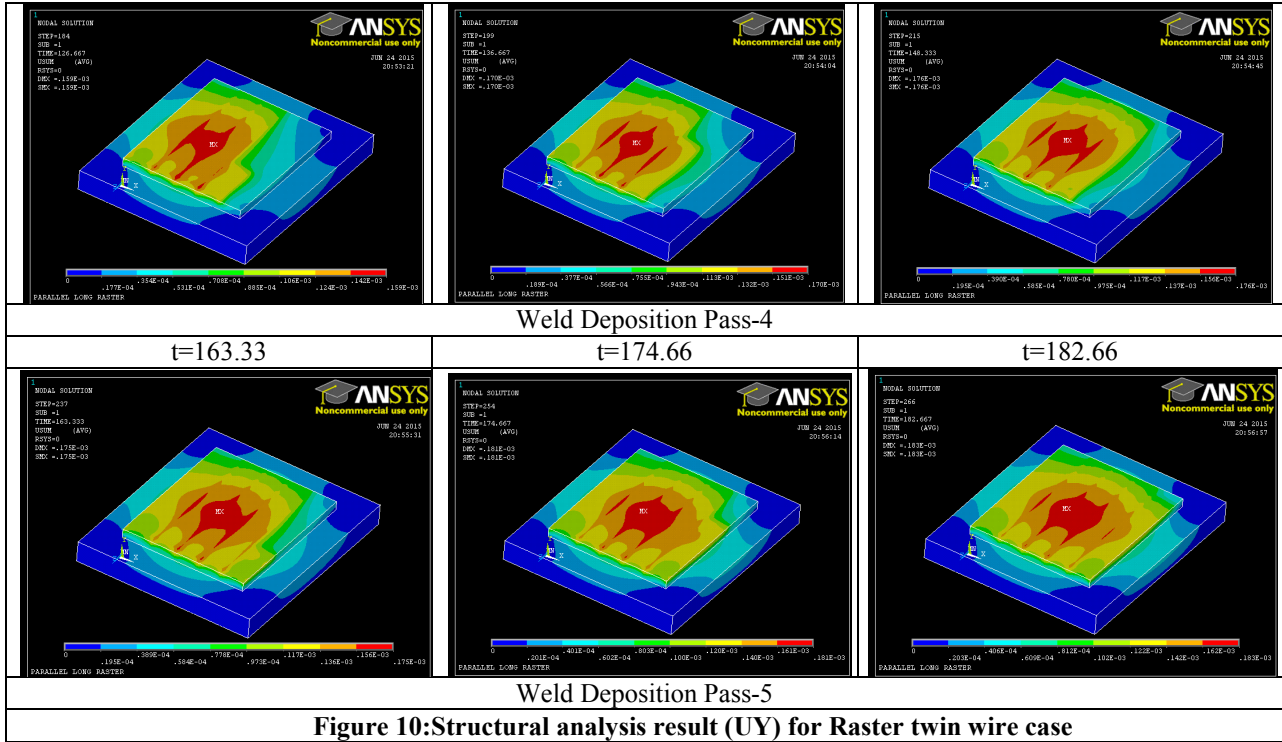
| | | |
|---|---|---|
|  |  |  |
| **Weld Deposition Pass-4** | | |
| t=163.33 | t=174.66 | t=182.66 |
|  |  |  |
| **Weld Deposition Pass-5** | | |
| **Figure 10:Structural analysis result (UY) for Raster twin wire case** | | |

| t=11.33 | t=24 | t=33.33 |
|---|---|---|
|  |  |  |
| **Weld Deposition Pass-1** | | |
| t=48.66 | t=61.33 | t=70.66 |
|  |  |  |
| **Weld Deposition Pass-2** | | |
| t=89.33 | t=96 | t=113.33 |

29

| Weld Deposition Pass-3 | | |
|---|---|---|
| t=126.66 | t=136.66 | t=148.33 |

| Weld Deposition Pass-4 | | |
|---|---|---|
| t=163.33 | t=174.66 | t=182.66 |

| Weld Deposition Pass-5 | | |
|---|---|---|

**Figure 11:Structural analysis result (SEQV) for Raster Twin wire case**
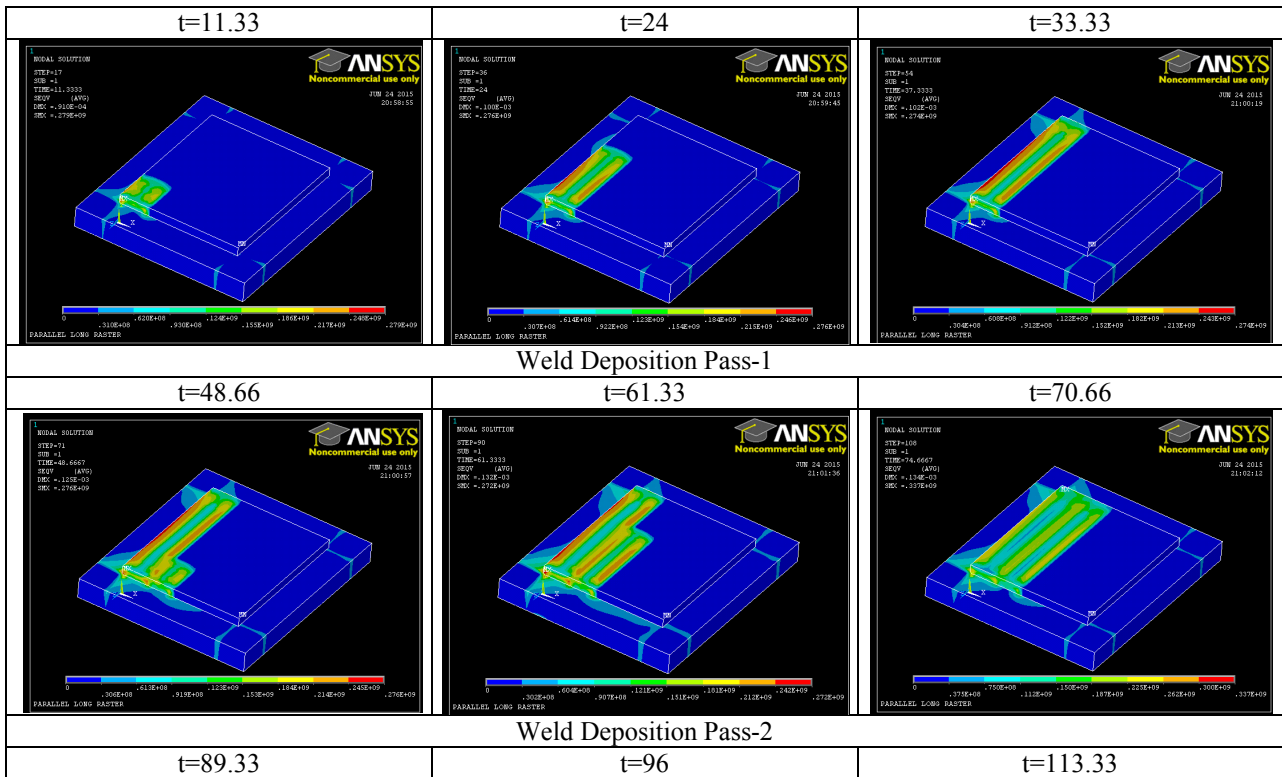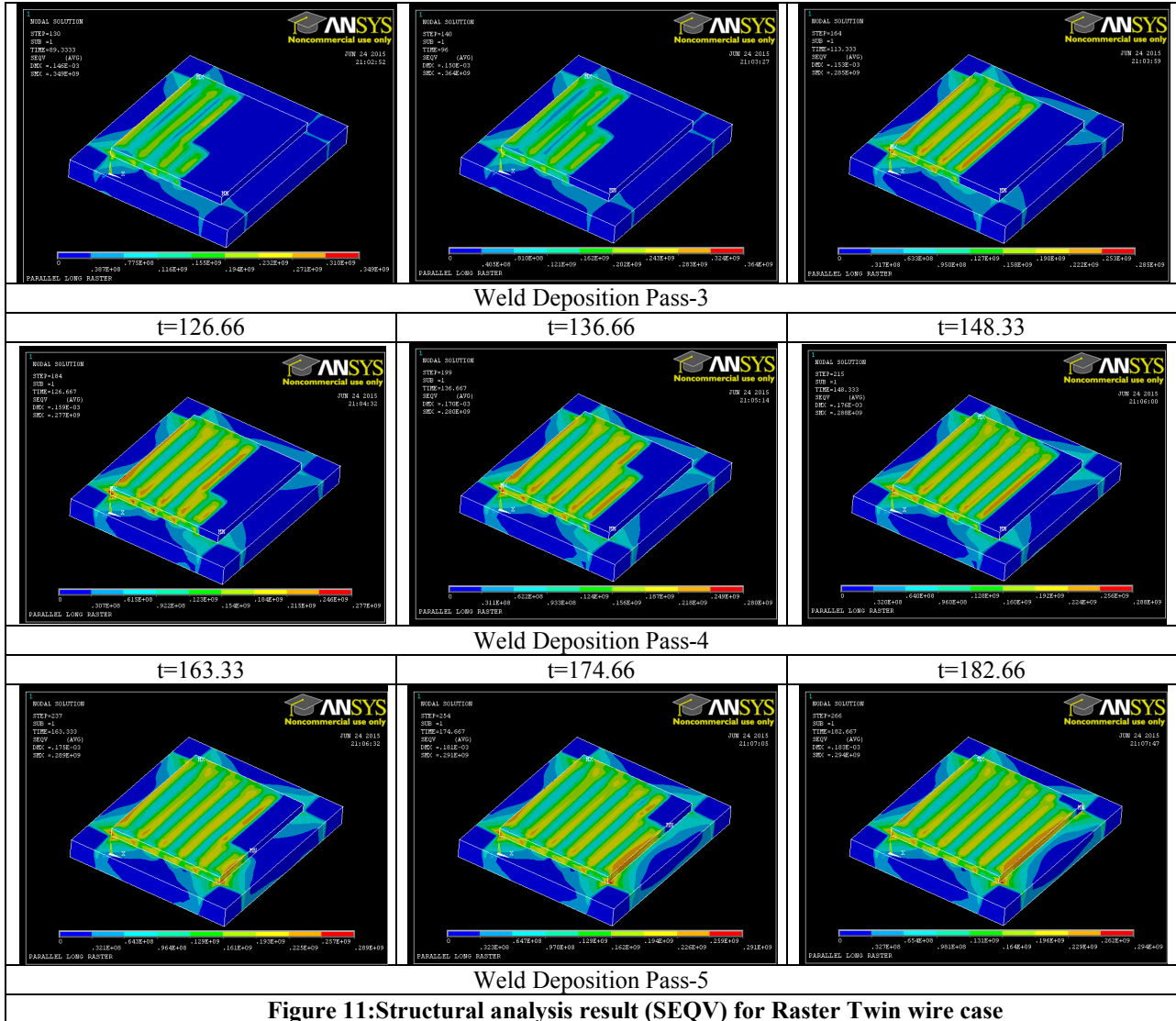
### 4.3.2 Zigzag Pattern

Thermal and Structural results for instance marked on Figure 12 for each pass/deposition are shown in Figure 13.
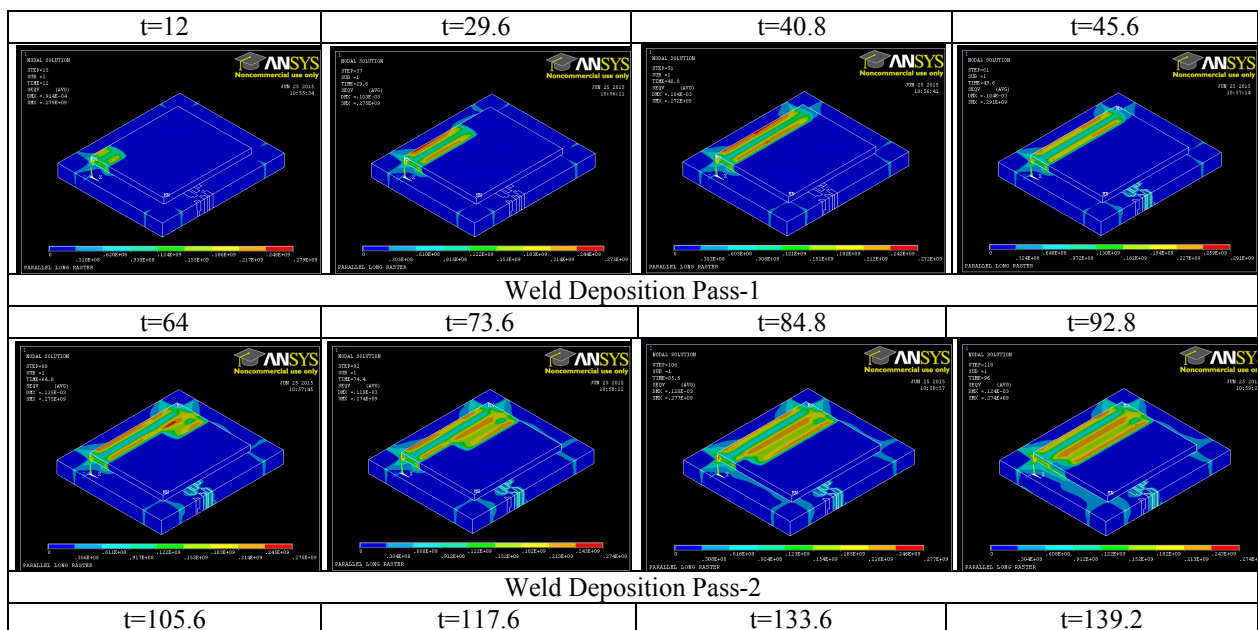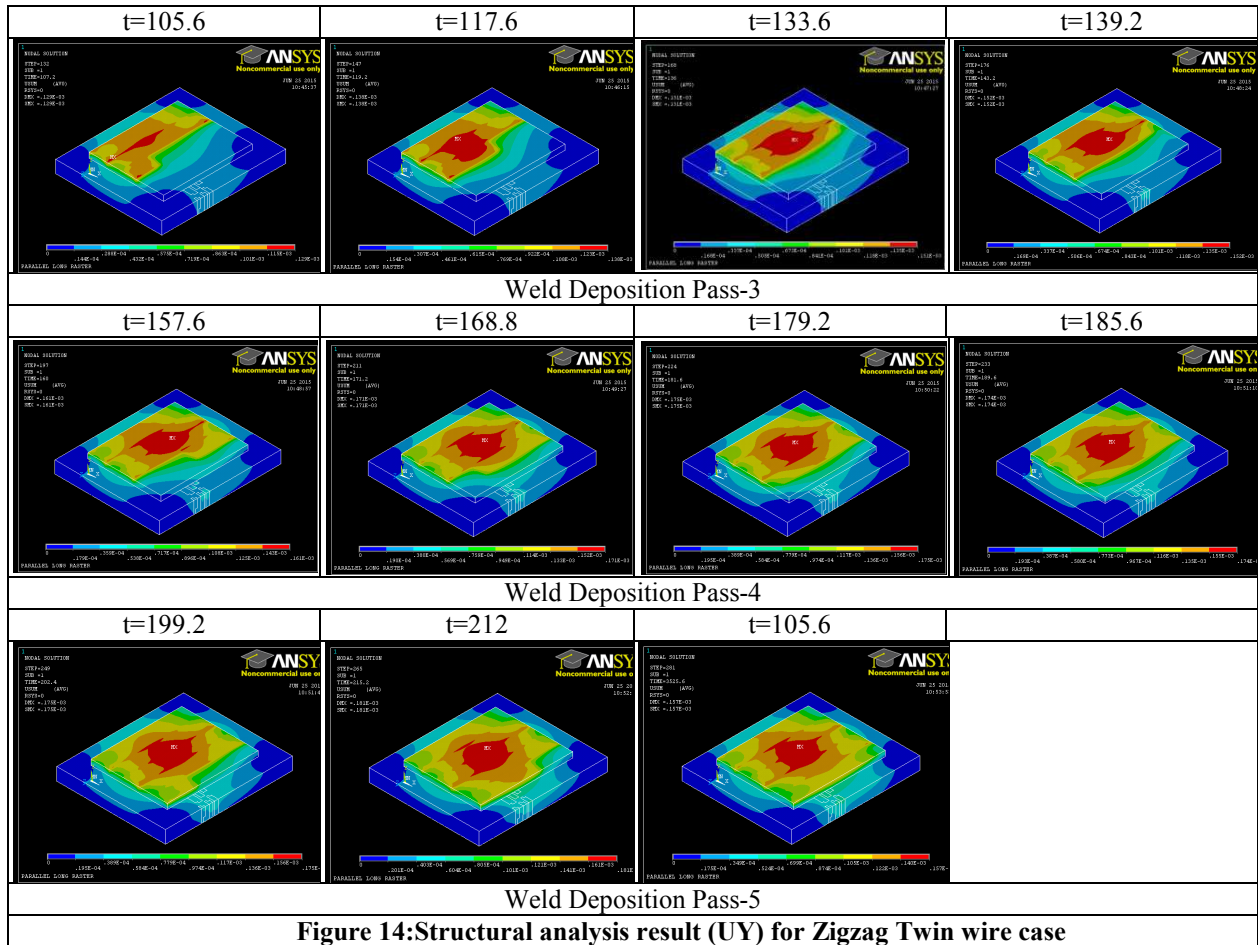
**Figure 12:Finite element mesh and Zigzag pattern**

| t=12 | t=29.6 | t=40.8 | t=45.6 |
|---|---|---|---|
|  |  |  |  |
| Weld Deposition Pass-1 | | | |
| t=64 | t=73.6 | t=84.8 | t=92.8 |
|  |  |  |  |
| Weld Deposition Pass-2 | | | |
| t=105.6 | t=117.6 | t=133.6 | t=139.2 |

| t=157.6 | t=168.8 | t=179.2 | t=185.6 |
|---------|---------|---------|---------|

Weld Deposition Pass-3

| t=199.2 | t=212 | t=105.6 | |
|---------|-------|---------|--|

Weld Deposition Pass-4

Weld Deposition Pass-5
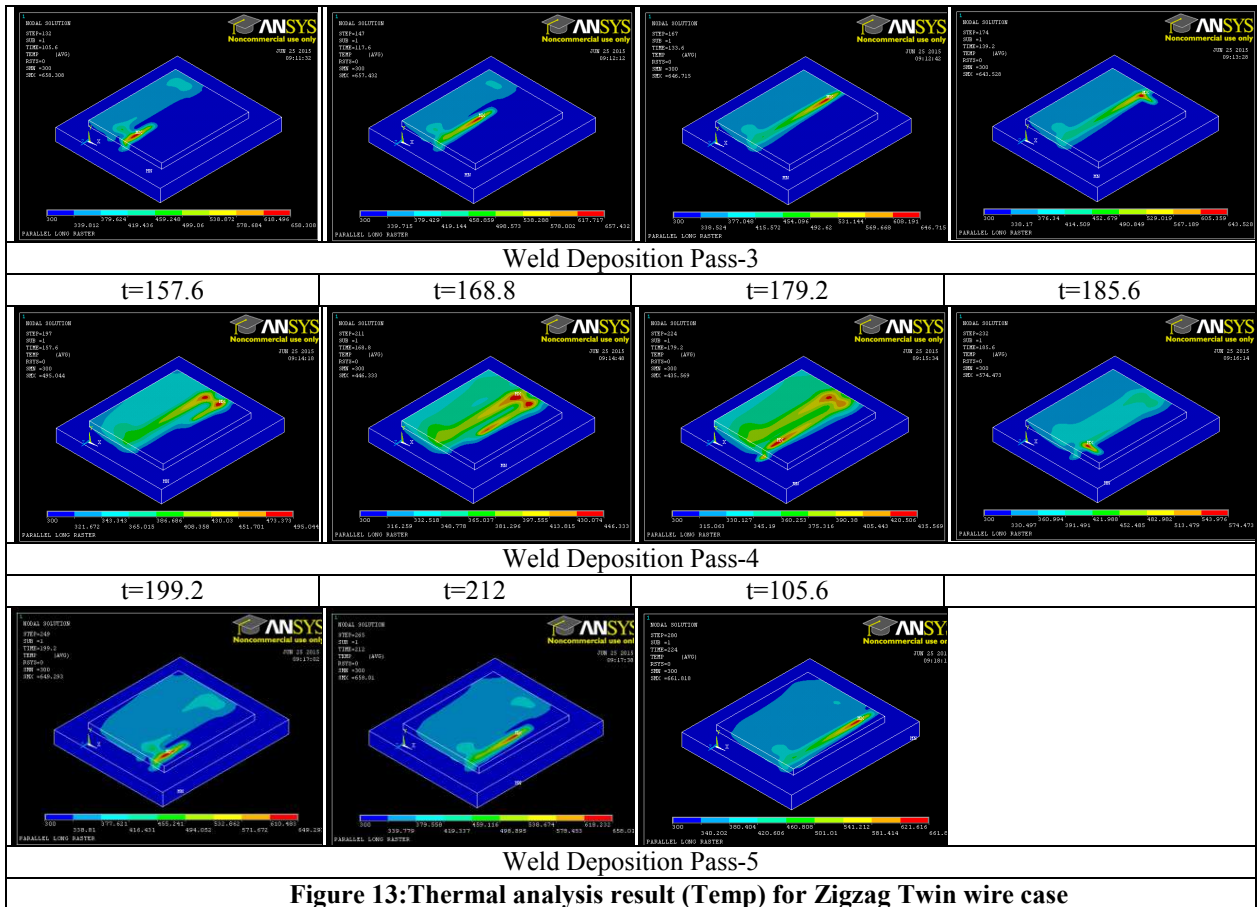
**Figure 13:Thermal analysis result (Temp) for Zigzag Twin wire case**

| t=12 | t=29.6 | t=40.8 | t=45.6 |
|------|--------|--------|--------|

Weld Deposition Pass-1

| t=64 | t=73.6 | t=84.8 | t=92.8 |
|------|--------|--------|--------|

Weld Deposition Pass-2

| t=105.6 | t=117.6 | t=133.6 | t=139.2 |
|---------|---------|---------|---------|
|  |  |  |  |
| Weld Deposition Pass-3 | | | |
| t=157.6 | t=168.8 | t=179.2 | t=185.6 |
|  |  |  |  |
| Weld Deposition Pass-4 | | | |
| t=199.2 | t=212 | t=105.6 | |
|  |  |  | |
| Weld Deposition Pass-5 | | | |
| **Figure 14:Structural analysis result (UY) for Zigzag Twin wire case** | | | |

| t=12 | t=29.6 | t=40.8 | t=45.6 |
|------|--------|--------|--------|
|  |  |  |  |
| Weld Deposition Pass-1 | | | |
| t=64 | t=73.6 | t=84.8 | t=92.8 |
|  |  |  |  |
| Weld Deposition Pass-2 | | | |
| t=105.6 | t=117.6 | t=133.6 | t=139.2 |

| t=157.6 | t=168.8 | t=179.2 | t=185.6 |
|---------|---------|---------|---------|

Weld Deposition Pass-3

| t=199.2 | t=212 | t=105.6 | |
|---------|-------|---------|--|

Weld Deposition Pass-4

Weld Deposition Pass-5

**Figure 15:Structural analysis result (SEQV) for Zigzag Twin wire case**

### 4.3.3 Spiral (Out-In) Pattern

Thermal and Structural results for instance marked on below image for each pass/deposition are shown subsequently.
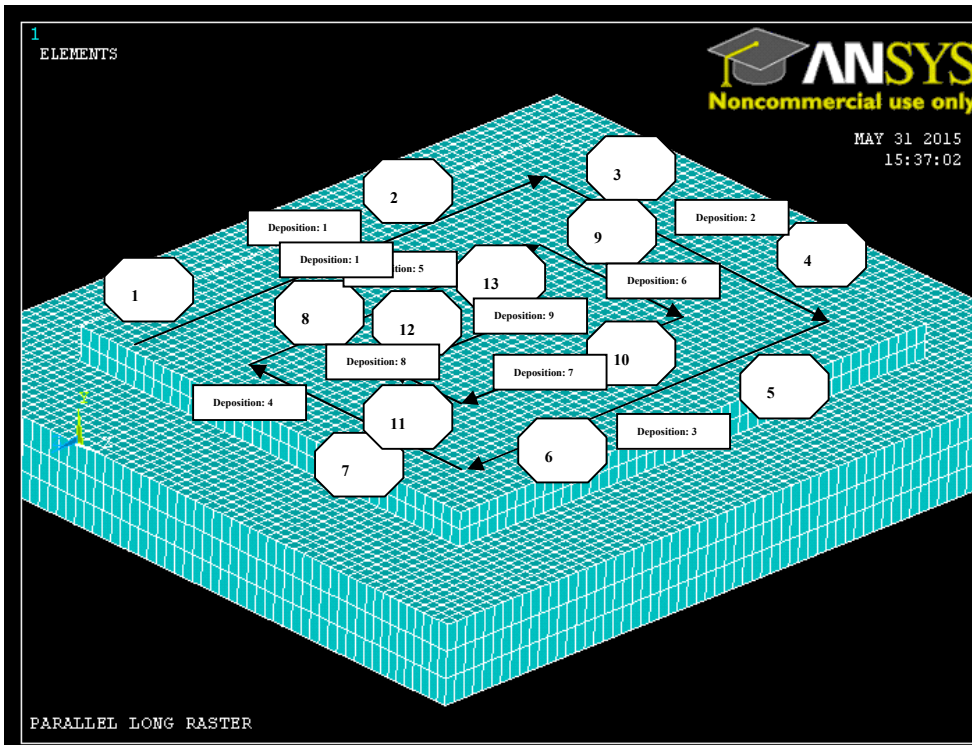
**Figure 16:Finite element mesh and Spiral (Out-IN) pattern**

| t=10 | t=10 | t=10 |
|------|------|------|
|  |  |  |
| Temp | UY | SEQV |
| t=27.33 | t=27.33 | t=27.33 |
|  |  |  |
| Temp | UY | SEQV |
| t=69 | t=69 | t=69 |

| | | |
|---|---|---|
|  |  |  |
| Temp | UY | SEQV |
| t=54 | t=54 | t=54 |
|  |  |  |
| Temp | UY | SEQV |
| t=70 | t=70 | t=70 |
|  |  |  |
| Temp | UY | SEQV |
| t=87.33 | t=87.33 | t=87.33 |
|  |  |  |
| Temp | UY | SEQV |
| t=100 | t=100 | t=100 |

| | | |
|:---:|:---:|:---:|
|  |  |  |
| Temp | UY | SEQV |
| t=121.33 | t=121.33 | t=121.33 |
|  |  |  |
| Temp | UY | SEQV |
| t=146 | t=146 | t=146 |
|  |  |  |
| Temp | UY | SEQV |
| t=165.33 | t=165.33 | t=165.33 |
|  |  |  |
| Temp | UY | SEQV |
| t=176 | t=176 | t=176 |

| | | |
|---|---|---|
| Temp | UY | SEQV |
| t=186.66 | t=186.66 | t=186.66 |
| Temp | UY | SEQV |
| t=188 | t=188 | t=188 |
| Temp | UY | SEQV |
| t=7088 | t=7088 | t=7088 |
| **Figure 17:Thermal and Structural Results for Spiral (Out-In)** | | |

## 4.4    Result Discussion

Results have been extracted along the cross Line 1 and 2 at the bottom face of substrate plate and top of weld bead.
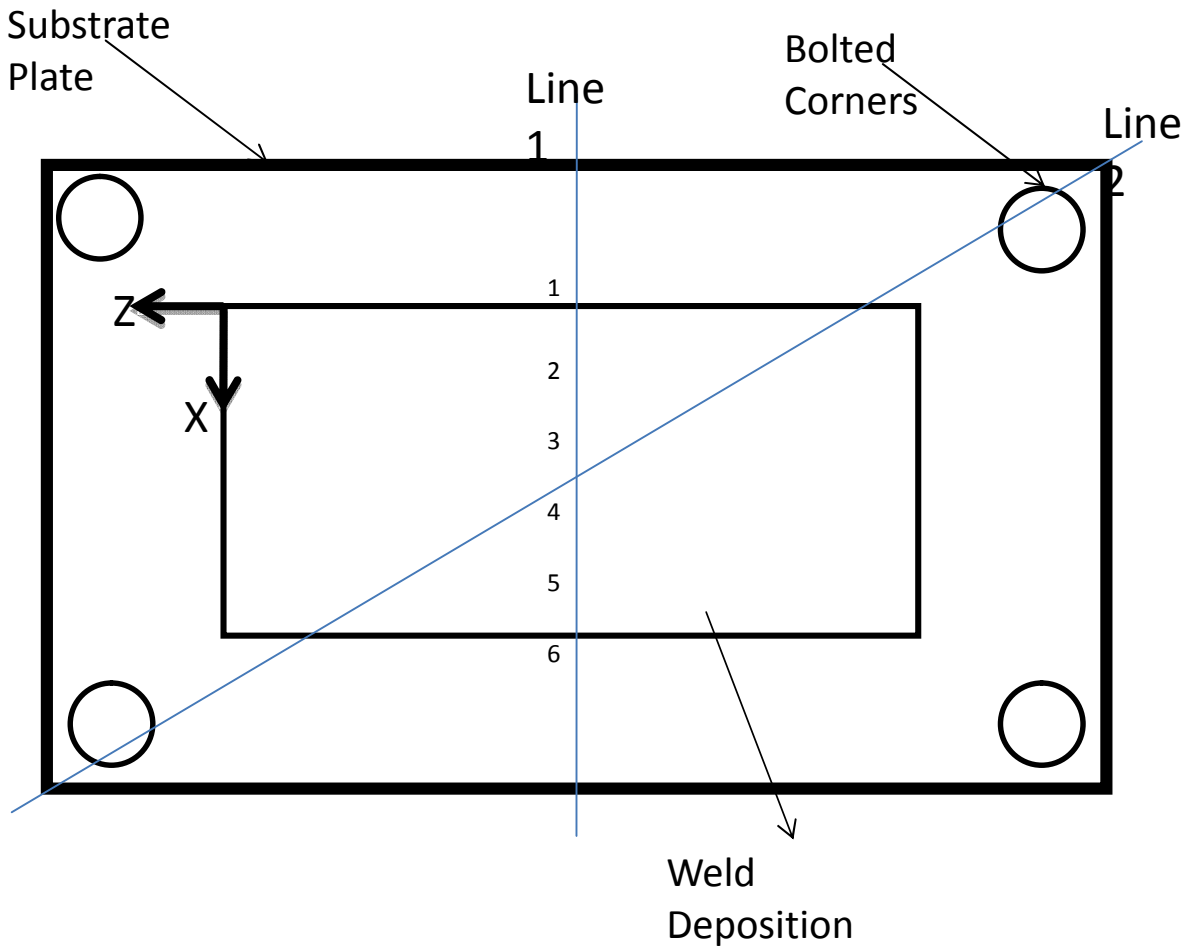


**Figure 18:Measurement Section (Line 1 and Line 2)**

### 4.4.1    Structural Result (Deformation)

The finite element simulation deflection along line 1 (Z=LD/2) are show in Figure 19 and 23 for raster pattern, Figure 25 and 29 for Zigzag pattern  and Figure 31 and  35 for spiral pattern on top and bottom. Similarly simulation deflection along line 2 (Diagonal) are show in Figure 21 for raster pattern, Figure 27 for Zigzag pattern and Figure 33 for spiral pattern on bottom. The location of the lines is shown in Figure 18. During deposition the thermal cycling results in

compressive reaction forces at the plate edges. This reaction forces cause the substrate plate to deflect upward. This upward deflection has a maximum at the mid-length of the plate and decreases on both the sides.

It is evident that the deflection is accumulative in nature as with each pass the deformation increases. The slope of the curve is determined by the relative position of the heat source. When the first few rows are being deposited the deflection increases very rapidly. But as the heat source moves to final few passes the rate of change of deflection slows down. The deflection of plate is due to the contraction forces arising from the shrinkage of molten metal and that of the substrate. As the effect of contraction forces, for first few passes will be larger therefore the initial rate of change in deflection is large.

### 4.4.2    Structural Result (Residual Stress)

The results are plotted along line 1 and line 2 at the bottom of substrate. Figure 20 and 22 shows results for raster pattern. Similarly Figure 26 and 28 shows results for Zigzag pattern and Figure 32 and 34show results for spiral pattern.

1.  **Raster Pattern:**
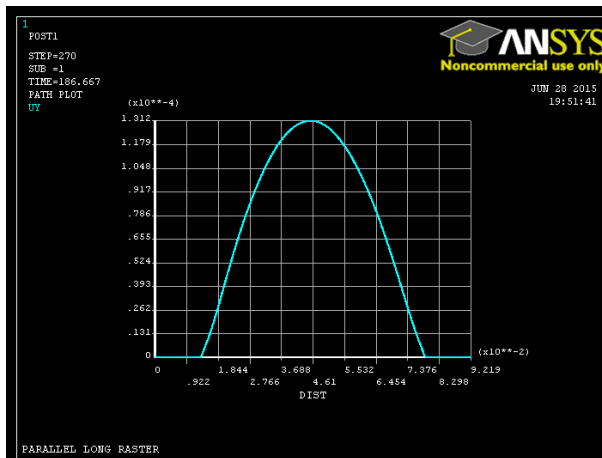


Figure 19: UY along line 1 (Bottom)        Figure 20: SEQV) along line 1 (Bottom
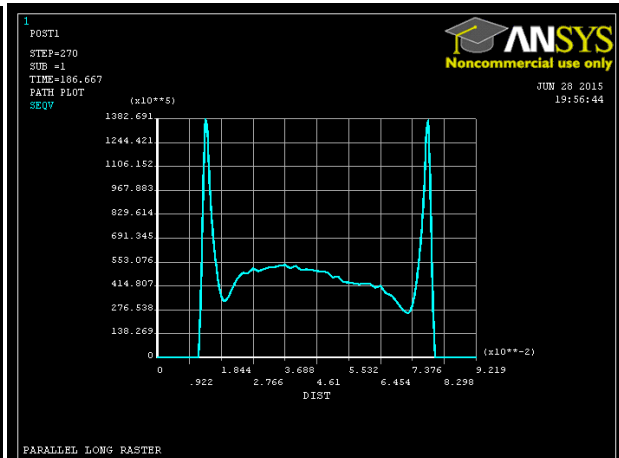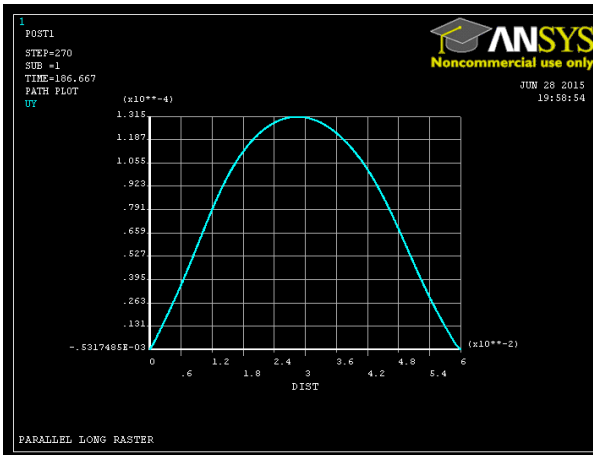
**Figure21: UY along line 2 (Bottom)**　　　　**Figure 22:SEQV along line 2 (Bottom)**
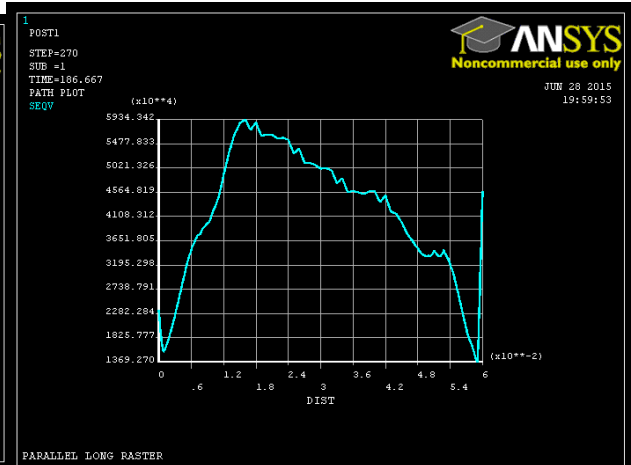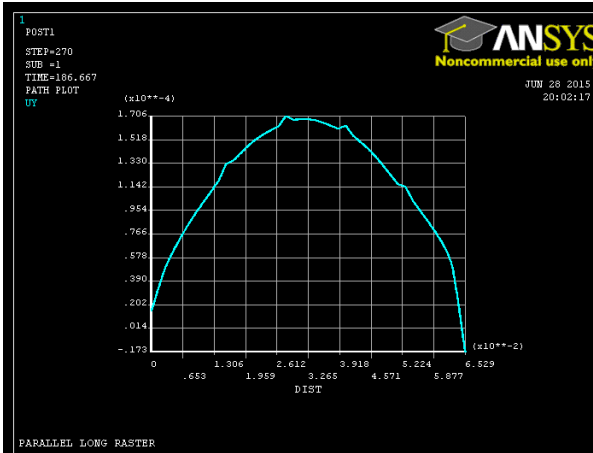




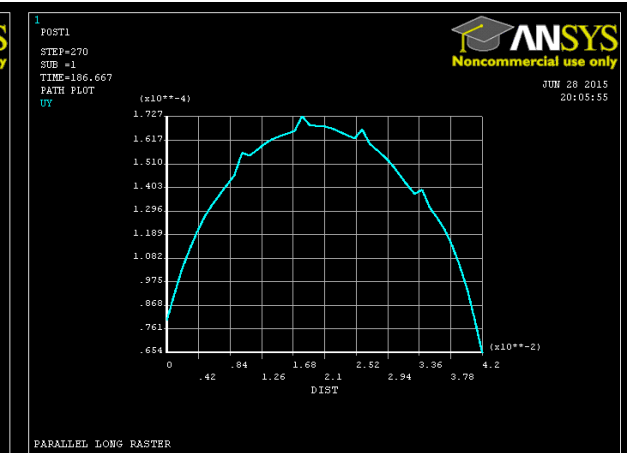**Figure 23: UY along line 1 (Top)**　　　**Figure 24: UY along line 2 (Top)**
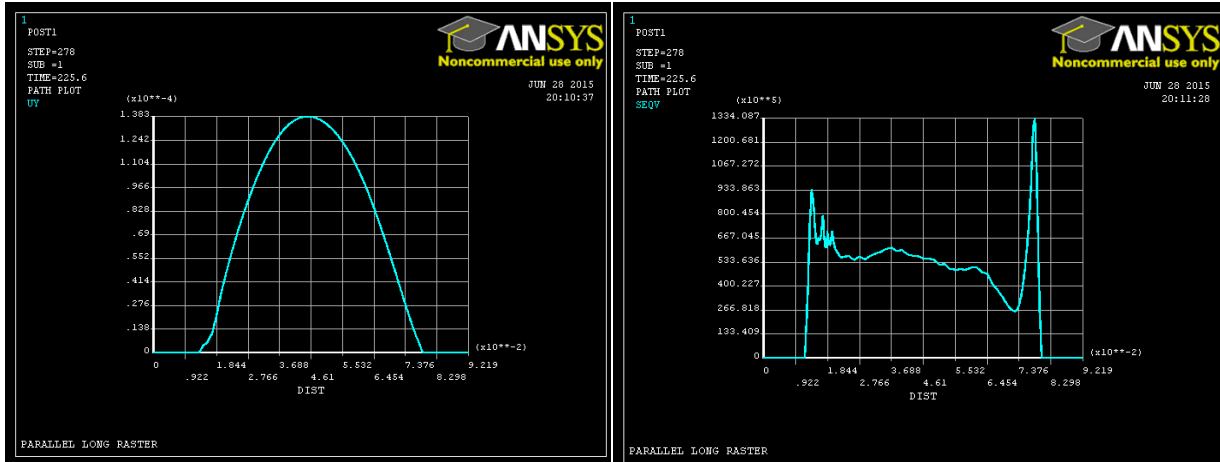
## 2. Zigzag Pattern:



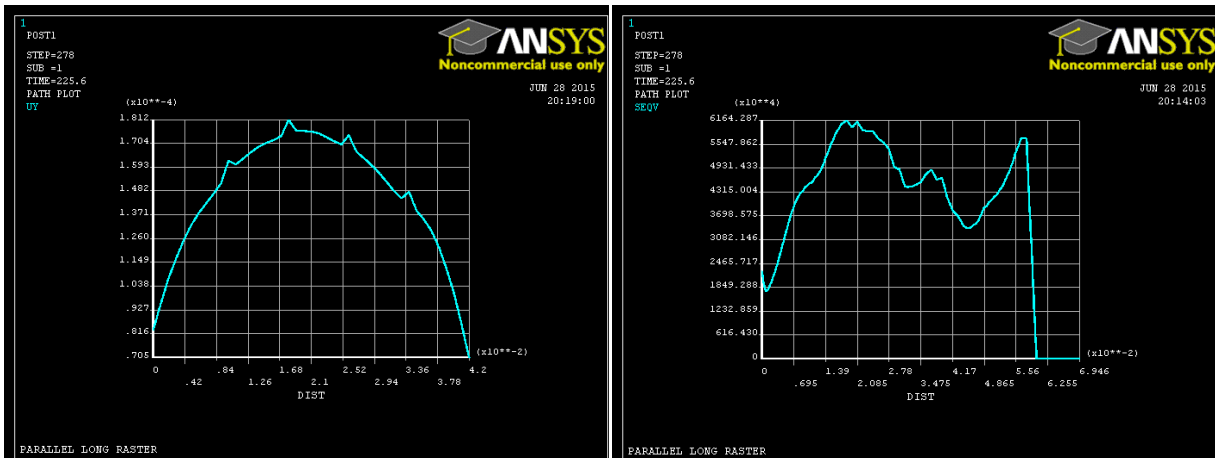**Figure 25: UY along line 1 (Bottom)    Figure 26:SEQV along line 1(Bottom)**



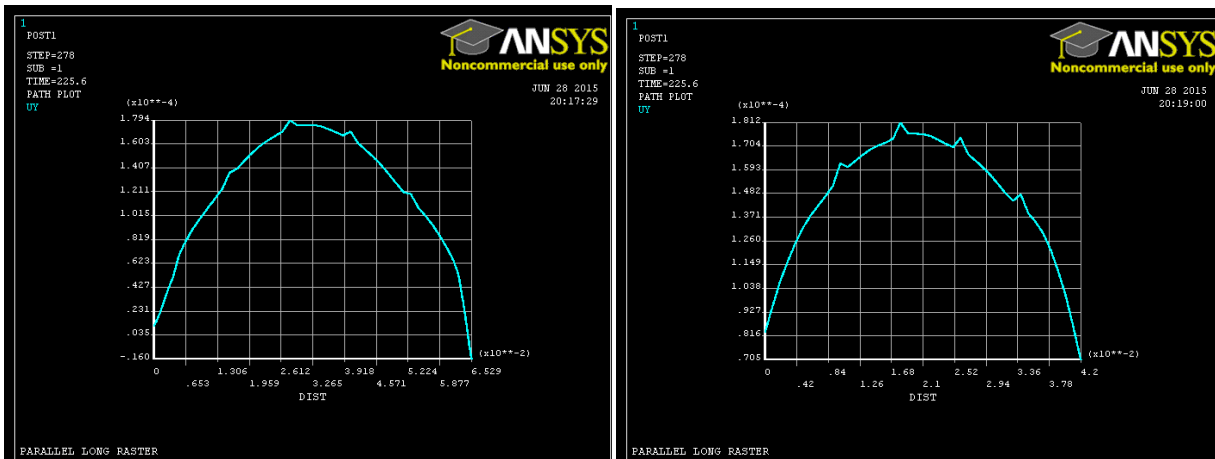**Figure 27: UY along line 2 (Bottom)  Figure 28:SEQV along line 2 (Bottom)**



**Figure 29: UYalong line 2 (Top)            Figure 30: UY along line 2 (Top)**
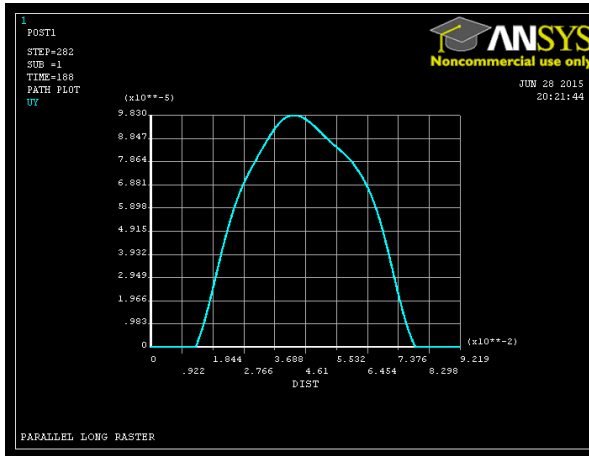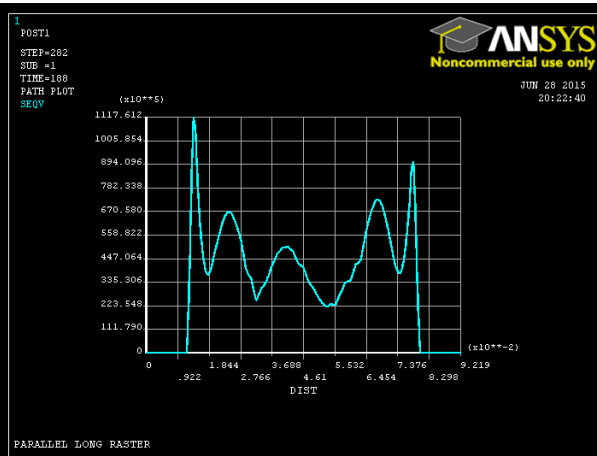
## 3. Spiral Pattern:



**Figure 31: UY along line 1 (Bottom)**


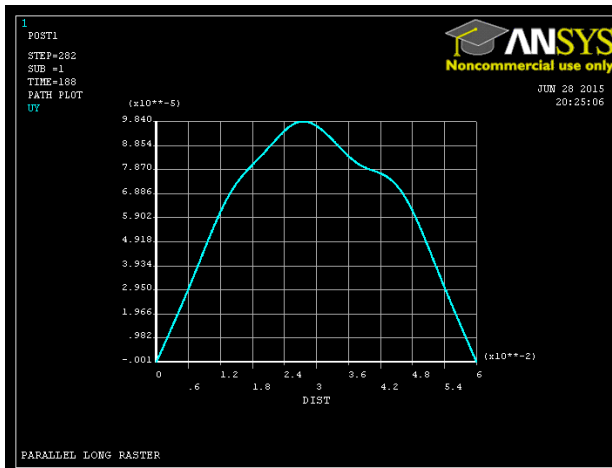
**Figure 32: SEQV along line 1 (Bottom)**


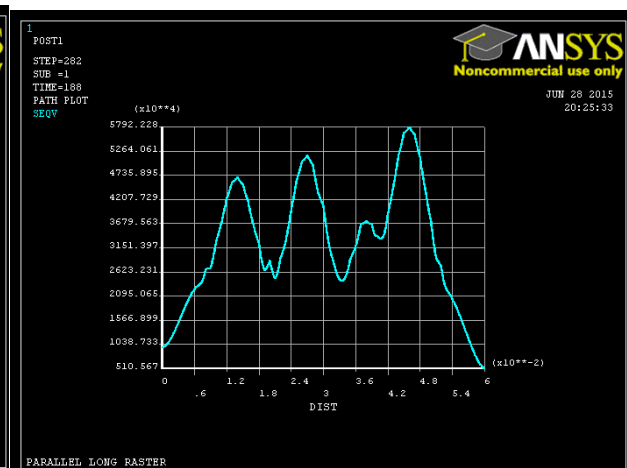
**Figure 33: UY along line 2 (Bottom)**



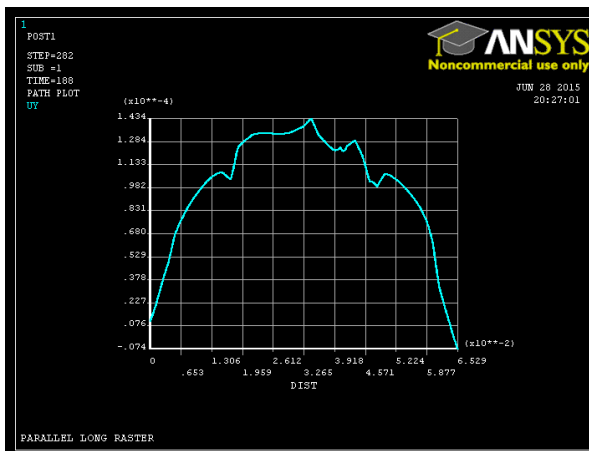**Figure 34: SEQV along line 2 (Bottom)**



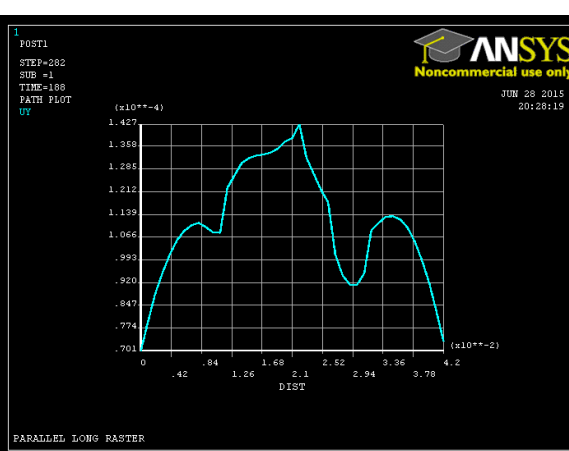**Figure 35: UY along line 1 (Top)**



**Figure 36: UY along line 2 (Top)**
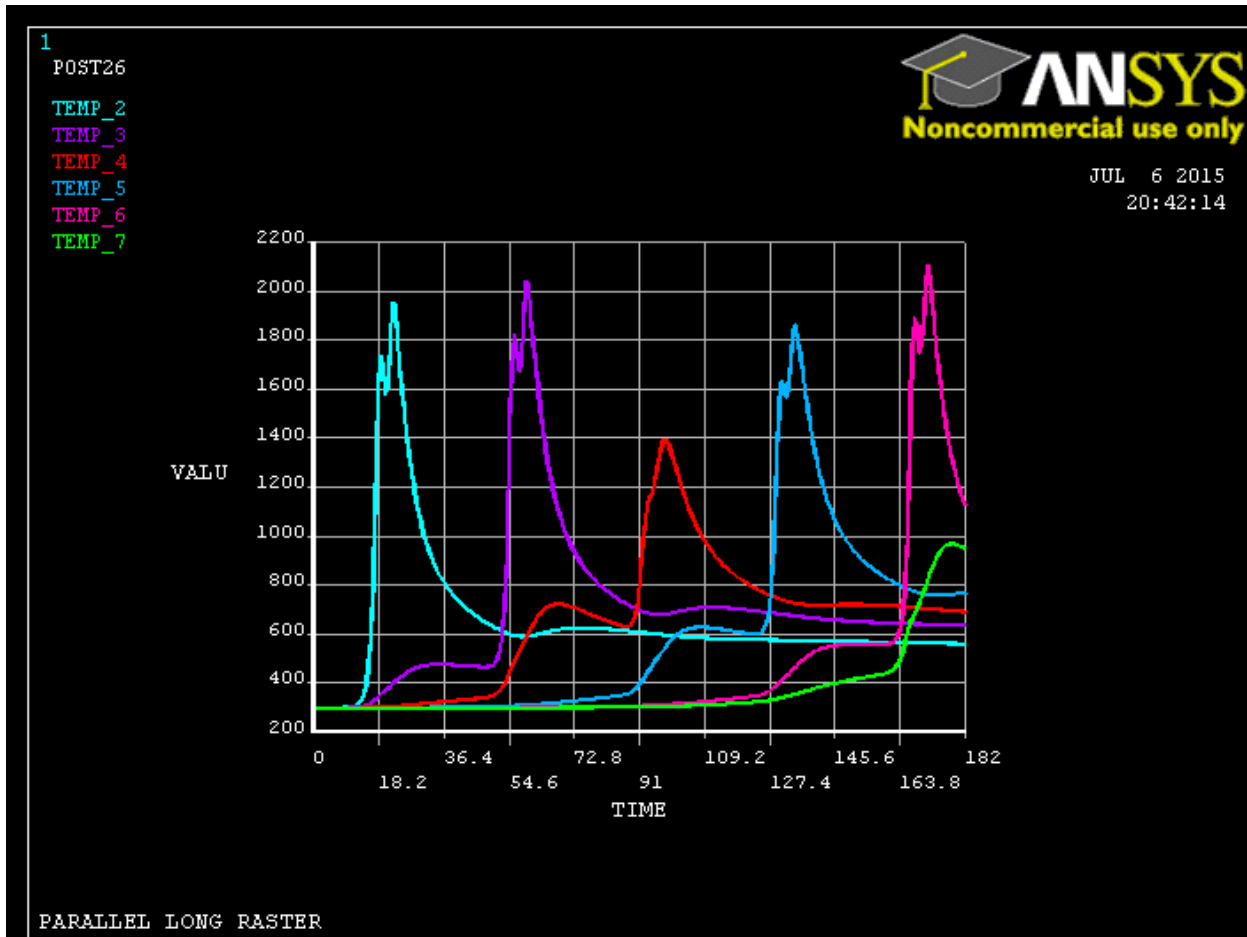
43

### 4.4.3 Thermal Result (Temp)



**Figure 35: Temp Vs Time for 6 equidistant points along line 1**

The temperature history of nodes lying at the intersection of substrate top and center-line of a bead is shown in figure. The positions of these nodes are shown in figure 18. The peak temperature for each point is same but the time at which this peak occurs is dissimilar. It is observed that when the heat source is close to any of the point under consideration, the temperature of that point is relatively higher therefore it can be concluded that the magnitude of thermal cycling is not symmetric but depends upon the relative position of the heat source.

# Chapter 5

# Conclusions and Future Scope

### 5.1 Conclusions

The application of metal arc welding as layered manufacturing technique is restricted to the build-up of large residual stresses and residual deformation. These problems must be minimized if metal arc welding is to be used as additive manufacturing method. In this chapter parametric simulation is performed to visualize the effect of various deposition sequences on the buildup of residual stresses and distortions.

In simulation deflection was found to be minimum for spiral pattern. But heat accumulation was observed at the middle. Also raster and Zigzag pattern give similar result for von-mises stresses i.e maximum at the start but decreases along bead direction. For spiral case von –mises distribution is uniform along bead direction.

### 5.2 Future Scope

Here Residual stress and deflection is studied for models made by three different deposition patterns. The study can be further progressed by studying the effect of relating the two or more patterns thereby managing the distribution of the thermally induced residual stress further.
The model can be extended easily to multiple layer study. And similar procedure can be used to model any specific geometry of the part.

Similarly effect of other parameters can be studied such as.

(1) Thermal Constraints:

    1. Welding speed (v)

    2. Wire feed rate (I & V)

(2) Deposition Parameters:

    1. Interpass cooling

2. Heat sink characteristics (Base plate material and constraints)

3. Number of beads for a layer

4. Deposition Sequence and Path

(3) Mechanical Constraints:

1. Edge Bolting

2. No Warping condition

# References

**Gebhardt, A.,** (2003) Rapid Prototyping, Hanser Gardner Publications, Inc., Cincinnati.

Kamrani, A.K. and Nasr, E. A. (2006), *Rapid Prototyping: Theory and Practice*, Springer,USA, ISBN: 9780387232904.

H. H. Zhao, H.C. Li, G. J. Zhang, Z. Q. Yin and L. Wu, Numerical Simulation of temperature field and stress distributions in multi pass-single layer weld based rapid prototyping.

Rizwan Alim Mufti **,**Mechanical and micro structural investigation of weld based rapid prototyping.

K.P. Karunakaran, Vishal Pushpa ,Sreenath Babu Akula ,Rajeev Dwivedi and R. Kovacevic,Techno-Economic Analysis of Hybrid Layered Manufacturing.

N. Keller, F. Neugebauer, H. Xu, V. Ploshikhin , Thermo-mechanical Simulation of Additive Layer Manufacturing  of Titanium Aerospace structures.

Hasan Fawad junejo , Finite Element modelling of weld based rapid prototyping.

A. Anca, V. Fachinotti and A. Cardona, Finite Element Modeling of shape deposition metal.

Bai-Qiao Chen, Prediction of Heating Induced Temperature Fields  and Distortions in Steel Plates.

Alexander H Nickel, Analysis of thermal stresses in shape deposition manufacturing metal parts.

# APPENDIX

A.  **Ansys Thermal APDL Code**

B.  **Ansys Structural APDL Code**